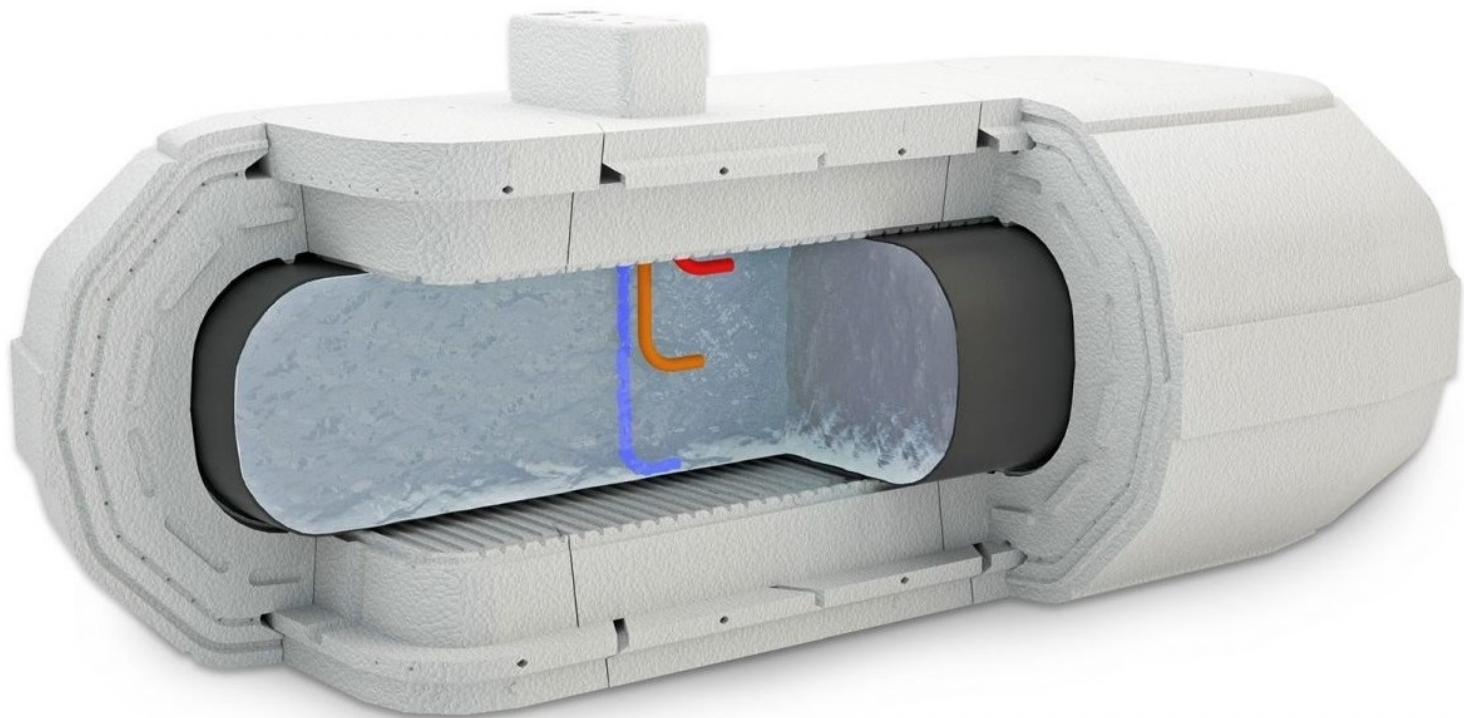


Analysing Thermal Energy Storage in Residential Buildings: Towards Decarbonization of the Heating Sector

Thesis MSc Sustainable Energy Technology

Celine van der Veen



ANALYSING THERMAL ENERGY STORAGE IN RESIDENTIAL
BUILDINGS: TOWARDS DECARBONIZATION OF THE HEATING
SECTOR

A thesis submitted to the Delft University of Technology in partial fulfilment
of the requirements for the degree of

Master of Science in Sustainable Energy Technology

by

Celine van der Veen

October 2022

C.M. van der Veen: *Analysing Thermal Energy Storage in Residential Buildings: Towards Decarbonization of the Heating Sector* (2022)

© This work is licensed under a Creative Commons Attribution 4.0 International License. To view a copy of this license, visit <http://creativecommons.org/licenses/by/4.0/>.

ISBN 999-99-9999-999-9

The work in this thesis was done in the following research group:



DC Systems, Energy Conversion & Storage
Department of Electrical Sustainable Energy
Faculty of Electrical Engineering, Mathematics and Computer Science
Delft University of Technology

Thesis committee: Prof. dr. P. Bauer
Dr. ir. L.M. Ramirez Elizondo
Dr. ir. M.J.B.M. Pourquoi
Daily supervisor: J.J. Alpizar Castillo

ABSTRACT

The majority of Dutch homes currently use natural gas boilers to meet their space heating demand. Changes in this significantly large sector are required to achieve the sustainability goals established by the Paris Agreement. Since most renewable energy sources produce electricity, transitioning residential heating systems might cause problems managing national electricity grids. Furthermore, the intermittent nature of renewable energy sources leads to an imbalance between supply and demand.

These challenges can be overcome by combining different storage techniques. An example of such a technique is the thermal energy buffer developed by Borg, which focuses on single-household use. This thesis looks into the feasibility of such a system by comparing different scenarios for residential heating systems.

Three scenarios were modelled using Simscape. In scenario I, a natural gas boiler provided all the heating demand of the house. In scenario II, the heating system consisted of Photovoltaic Thermal (PVT) panels and the thermal energy buffer. In scenario III, the house was heated by PVT panels, the thermal energy buffer, and a heat pump. In all scenarios, the same house was connected to the heating system.

In scenario II, the system sizes were 0, 1, 2, and 3 PVT panels, combined with buffer capacities of 0, 2, 4, and 6 m³. In scenario III, the system sizes were: 3 PVT panels with 6 m³ buffer capacity, 1 PVT panel with 4 m³ buffer capacity, and 3 PVT panels with 2 m³ buffer capacity.

The total yearly heat consumption of the modelled house was 5109 kWh. In scenario I, 378 kg of CO₂ was emitted. In scenario II, CO₂ emissions were highly dependent on the sizing of the PVT system and the TESS and ranged from 20 to 405 kg, based on a heating demand of 9444 kWh.

Scenarios I and III maintained a comfortable temperature during the entire year. The heating system of scenario II was insufficient to heat the house throughout the year for all modelled system sizes; however, the scenario could be acceptable with larger PVT and TESS sizing. By comparing CO₂ emissions and payback time, the optimal capacity of the thermal energy buffer was found to be 6 m³.

The uncertainty of the future gas price causes a challenge in comparing the cost of electrified heating systems to traditional heating systems. Additionally, it underlines the necessity of decarbonizing residential heating systems to secure comfortable, affordable housing.

PREFACE

This research, in the context of my master thesis, is the result of my time as a student at TU Delft, particularly as an MSc Sustainable Energy Technology student. There are a few people whom I want to thank especially for helping me during my thesis.

Joel, my PhD supervisor, I want to thank you for your extensive guidance inside and outside our weekly meetings. For brainstorming about my project, our frustrating but helpful Simulink debugging sessions, and your encouraging chocolates afterwards :)

Laura Ramirez Elizondo, I want to thank you for giving me the opportunity to do my thesis at DCE&S and for the monthly meetings and feedback.

I also want to thank my other thesis committee members, Pavol Bauer and Mathieu Pourquie, for their quick responses to my questions.

Finally, I thank my friends and family for your mental support and distractions. In particular, I would like to thank Anouk for all our productive study sessions at EEMCS, 'gezellige' coffee breaks, and 'treat yourself' moments. Lastly, I would like to thank Pieter for pre-reading my thesis report and for your mental support during this process.

Celine van der Veen

CONTENTS

Abstract	v
Preface	vii
List of Figures	5
List of Tables	7
List of Acronyms	9
1 INTRODUCTION	11
2 THEORY	13
2.1 Heat Transfer	13
2.2 Residential Heating Technologies	13
2.2.1 Gas Boiler	14
2.2.2 Heat Pump	14
2.2.3 Photovoltaic Thermal Modules	17
2.2.4 Infrared Panels	19
2.2.5 Comparison of Heating Technologies	19
2.3 Thermal Energy Storage	20
2.3.1 Types of Thermal Energy Storage	21
2.3.2 Thermal Energy Storage Tanks	21
2.4 Thermal Energy Distribution	22
2.4.1 Pipes	22
2.4.2 Valves	23
2.4.3 Heat Pipes	24
2.5 Thermal Losses in a Residential Building	24
2.6 Heating Electrification Effects on House Power Networks	25
3 METHODOLOGY	27
3.1 Heating System Scenarios	27
3.2 Data	27
3.3 Models	28
3.3.1 Residential Heating System	28
3.3.2 Scenario I: Boiler	30
3.3.3 Scenario II: PVT + TESS	31
3.3.4 Scenario III: PVT + TESS + HP	34
4 RESULTS	37
4.1 Scenario I: Boiler	37
4.1.1 Fuel Costs	38
4.2 Scenario II: PVT + TESS	38
4.2.1 Payback Time	40
4.3 Scenario III: PVT + TESS + HP	41
5 DISCUSSION	45
5.1 Model limitations	45
5.1.1 Residential Heating System	45
5.1.2 Instability of the Natural Gas Price	46
5.1.3 TESS	46
5.2 Comparing Scenarios I, II and III	47
5.3 Optimal Buffer Capacity	47
5.4 TESS Installation Requirements	48
6 CONCLUSIONS	49
Bibliography	54
A HOUSE PARAMETERS	55
B ADDITIONAL RESULTS SCENARIO I	57
C ADDITIONAL RESULTS SCENARIO II	59

D	ADDITIONAL RESULTS SCENARIO III	71
E	PVT MODULE PARAMETERS	73

LIST OF FIGURES

Figure 2.1	The components of a gas boiler. Adapted from [11].	14
Figure 2.2	Heat pump principles.	15
Figure 2.3	The fraction (in red) of the solar spectrum (in yellow) that can be converted into electrical energy by a c-Si solar cell. Taken from [9].	17
Figure 2.4	The components of a PVT collector. Taken from [21].	18
Figure 2.5	Infrared panel heating.	19
Figure 2.6	Thermal stratification in a storage tank, separating water into different thermal regions: hot, thermocline and cold. Taken from [36].	22
Figure 2.7	An infinitesimal section of a pipe.	22
Figure 2.8	Different valve types. Adapted from [40].	23
Figure 2.9	A schematic overview of a heat pipe. Taken from [43].	24
Figure 2.10	A schematic overview of the different components playing a role in heat transfer through a flat plate such as a wall or window.	25
Figure 3.1	A representation of the three different system architectures. From left to right, the systems are (I) a boiler system, (II) a combined PVT and buffer system, and (III) a system with a PVT, buffer and heat pump.	27
Figure 3.2	The heat flow in a residential building as modelled in Simulink. Yellow lines represent the thermal liquid domain, and orange lines represent the thermal domain.	28
Figure 3.3	The radiator subsystem. Yellow lines represent the thermal liquid domain, and orange lines represent the thermal domain.	28
Figure 3.4	The room subsystem contains the thermal losses through walls, roof, and windows.	29
Figure 3.5	This Simulink model simulates a house with a traditional heating system.	30
Figure 3.6	The control subsystem.	30
Figure 3.7	The heater subsystem. Yellow lines represent the thermal liquid domain, orange lines represent the thermal domain, and green lines represent the mechanical rotational domain.	31
Figure 3.8	This Simulink model simulates a house with a heating system consisting of a PVT system and a TESS.	31
Figure 3.9	A flowchart representing the control strategy of the model.	32
Figure 3.10	The PVT subsystem.	32
Figure 3.11	The TESS subsystem.	33
Figure 3.12	The Borg thermal energy storage tank prototype that is installed in The Green Village on the TU Delft campus. Taken from [6].	34
Figure 3.13	This Simulink model simulates a house with a heating system consisting of a PVT system, TESS, and HP.	35
Figure 3.14	The implemented heat pump load curve. The y-axis shows the heat load of the condenser in W, which is the heat output of the heat pump. The x-axis shows the time in minutes.	35
Figure 4.1	Yearly temperature variation in scenario I.	37
Figure 4.2	Seasonal temperature variation in scenario I.	38
Figure 4.3	The cumulative cost curve for an entire year.	38

Figure 4.4	The number of uncomfortable days for each system size in a year.	39
Figure 4.5	The yearly temperature variation for 1 PVT panel and 4 m ³ TESS capacity.	39
Figure 4.6	The yearly temperature variation for 3 PVT panels and 6 m ³ TESS capacity.	39
Figure 4.7	The seasonal temperature variation for 1 PVT panel and 4 m ³ TESS capacity.	40
Figure 4.8	The seasonal temperature variation for 3 PVT panels and 6 m ³ TESS capacity.	40
Figure 4.9	The years of payback time for each heating system size.	41
Figure 4.10	The CO ₂ emissions for each heating system size.	41
Figure 4.11	The yearly temperature variation for 3 PVT panels, 6 m ³ TESS capacity, and a heat pump.	42
Figure 4.12	The seasonal temperature variation for 3 PVT panels, 6 m ³ TESS capacity, and a heat pump.	42
Figure 4.13	The total thermal energy exchanged by the TESS on each day of the year for 3 PVT panels, 6 m ³ TESS capacity, and a heat pump.	43
Figure 4.14	The ratio of thermal energy generated by the PVT panels that is wasted on each day of the year for 3 PVT panels, 6 m ³ TESS capacity, and a heat pump.	43
Figure 5.1	Average natural gas price for Dutch consumers. Data taken from [27].	46
Figure 5.2	Heat distribution diagram in the modelled residential building.	48
Figure 5.3	Power distribution diagram in the modelled residential building.	48
Figure B.1	Simulink model for scenario I based on mass flow input data.	57
Figure B.2	Data input.	57
Figure B.3	Yearly outdoor and resulting indoor temperature variation.	58
Figure B.4	Monthly temperature variation in January.	58
Figure C.1	The yearly temperature variation for 0 PVT panels and 0 m ³ TESS capacity.	59
Figure C.2	The seasonal temperature variation for 0 PVT panels and 0 m ³ TESS capacity.	59
Figure C.3	The yearly temperature variation for 1 PVT panel and 0 m ³ TESS capacity.	60
Figure C.4	The seasonal temperature variation for 1 PVT panel and 0 m ³ TESS capacity.	60
Figure C.5	The yearly temperature variation for 1 PVT panel and 2 m ³ TESS capacity.	61
Figure C.6	The seasonal temperature variation for 1 PVT panel and 2 m ³ TESS capacity.	61
Figure C.7	The yearly temperature variation for 1 PVT panel and 6 m ³ TESS capacity.	62
Figure C.8	The seasonal temperature variation for 1 PVT panel and 6 m ³ TESS capacity.	62
Figure C.9	The yearly temperature variation for 2 PVT panels and 0 m ³ TESS capacity.	63
Figure C.10	The seasonal temperature variation for 2 PVT panels and 0 m ³ TESS capacity.	63
Figure C.11	The yearly temperature variation for 2 PVT panels and 2 m ³ TESS capacity.	64
Figure C.12	The seasonal temperature variation for 2 PVT panels and 2 m ³ TESS capacity.	64

Figure C.13	The yearly temperature variation for 2 PVT panels and 4 m ³ TESS capacity.	65
Figure C.14	The seasonal temperature variation for 2 PVT panels and 4 m ³ TESS capacity.	65
Figure C.15	The yearly temperature variation for 2 PVT panels and 6 m ³ TESS capacity.	66
Figure C.16	The seasonal temperature variation for 2 PVT panels and 6 m ³ TESS capacity.	66
Figure C.17	The yearly temperature variation for 3 PVT panels and 0 m ³ TESS capacity.	67
Figure C.18	The seasonal temperature variation for 3 PVT panels and 0 m ³ TESS capacity.	67
Figure C.19	The yearly temperature variation for 3 PVT panels and 2 m ³ TESS capacity.	68
Figure C.20	The seasonal temperature variation for 3 PVT panels and 2 m ³ TESS capacity.	68
Figure C.21	The yearly temperature variation for 3 PVT panels and 4 m ³ TESS capacity.	69
Figure C.22	The seasonal temperature variation for 3 PVT panels and 4 m ³ TESS capacity.	69
Figure D.1	The yearly temperature variation for 3 PVT panels, 2 m ³ TESS capacity and a heat pump.	71
Figure D.2	The seasonal temperature variation for 3 PVT panels, 2 m ³ TESS capacity and a heat pump.	71
Figure D.3	The yearly temperature variation for 1 PVT panel, 4 m ³ TESS capacity and a heat pump.	72
Figure D.4	The seasonal temperature variation for 1 PVT panel, 4 m ³ TESS capacity and a heat pump.	72

LIST OF TABLES

Table 2.1	Several available refrigerants [18]. The boiling and freezing point are given at p_{atm} and can be increased by applying higher operating pressure.	16
Table 2.2	A comparing table on different heating technologies.	20
Table 2.3	The calculated LCOE of different heating technologies.	20
Table 3.1	Properties of the Borg buffer prototype [6]	33
Table 3.2	An estimation for the initial costs for PVT modules and a TESS.	34
Table A.1	House parameters considering the walls.	55
Table A.2	House parameters considering the windows.	55
Table A.3	House parameters considering the roof.	55
Table E.1	PVT module parameters	73

LIST OF ACRONYMS

TES	Thermal Energy Storage	19
COP	Coefficient of Performance	16
PVT	Photovoltaic Thermal	17
SHS	Sensible Heat Storage	21
LHS	Latent Heat Storage	21
THS	Thermochemical Heat Storage	21
TTES	Tank Thermal Energy Storage	21
PTES	Pit Thermal Energy Storage	21
ATES	Aquifer Thermal Energy Storage	21
BTES	Borehole Thermal Energy Storage	21
LCOE	Levelised Cost of Energy	20
SPF	Seasonal Performance Factor	16
SCOP	Seasonal Coefficient of Performance	16
PV	Photovoltaic	17
TESS	Thermal Energy Storage System	27
DHW	Domestic Hot Water	45
HP	Heat Pump	27
STC	Standard Test Conditions	17
SOC	State of Charge	33

1

INTRODUCTION

In 2018, as much as 13% of the total Dutch final energy consumption was used for residential space heating [1]. Currently, 93% of households meet their space heating demand with natural gas boilers [2]. Changes in this significantly large sector are essential to reach the set sustainability goals by the Paris Agreement.

Since most renewable energy sources generate electricity, transitioning to a sustainable energy system may involve issues in the grid management of national electricity systems [3]. For example, Rüdüsüli [4] advised to “conduct investigations on tangible building flexibility options, such as local and district heat storage and storage options on both sides of heat pumps (electricity or heat)”. Substantial amounts of imported electricity are required in winter without adding storage options to an electrified energy system. At the same time, there is a surplus of energy generation in summer caused by photovoltaics [5].

The solution to these problems is to combine different storage techniques. One of these techniques is Thermal Energy Storage (TES), specifically, Tank Thermal Energy Storage (TTES). Borg [6] developed a prototype for such a tank, operating as a thermal energy buffer for a single household. This thesis looks into the feasibility of such a system by answering the research questions below.

Research Questions

- What are the requirements to make a residential heating system compatible with a thermal energy buffer?
- What is the optimal way of using a thermal energy buffer in terms of storage and consumption conditions to minimise costs?
- What are the differences in energy use of households that generate thermal energy for space heating (I) using a traditional heating system with a boiler, (II) with Photovoltaic Thermal (PVT) modules and a thermal buffer and (III) with PVT modules, thermal buffer and heat pump?
- Considering volumetric constraints, what is the optimal capacity of a thermal energy buffer that minimises costs and CO₂ emissions?

Report Structure

This paragraph describes the format of the report. First of all, Chapter 2 explains the critical theory to understand the different aspects of the project. Secondly, Chapter 3 explains the methods used to answer the research questions. Afterwards, the results are presented in Chapter 4, and these will be analysed in Chapter 5, along with research limitations. Finally, Chapter 6 presents the conclusions of this research, along with recommendations for further study. In addition to these chapters, the report contains appendices with further information.

2 | THEORY

This Chapter contains a thorough literature review on the relevant background of the research, which is crucial for interpreting this report's results. First of all, heat transfer basics will be explained in Section 2.1. Afterwards, different heating techniques will be presented and compared in Section 2.2. Next, the necessity for thermal energy storage will be justified in Section 2.3, along with an explanation of thermal energy storage tanks. Finally, the distribution of thermal energy will be described in Section 2.4.

2.1 HEAT TRANSFER

Heat transfer is the transportation of thermal energy due to spatial temperature differences [7]. There are three types of heat transfer: conduction, convection and radiation. This Section will elaborate on these types of heat transfer.

Conductive heat transfer is the capacity of molecules to transport thermal energy without net mass transport [8]. Fourier's Law in Equation 2.1 describes this phenomenon [9].

$$\frac{dQ}{dt} = -kA \frac{dT}{dx} \quad (2.1)$$

In this Equation, dQ/dt is the thermal energy flow in J/s, k is the thermal conductivity coefficient of the material in W/mK, A is the area of contact in m^2 , and dT/dx is the temperature gradient in the material in K/m.

Convective heat transfer is the transfer of thermal energy by the motion of a fluid or gas. It can be described by Newton's Law of Cooling in Equation 2.2 [8].

$$\frac{dQ}{dt} = -hA\Delta T \quad (2.2)$$

In this Equation, dQ/dt is the thermal energy flow in J/s, h is the heat transfer coefficient of the medium in W/m^2K and ΔT is the temperature difference in K between the two points of interest.

Radiative heat transfer transfers thermal energy by photons or electromagnetic radiation. Every object emits a certain quantity of electromagnetic radiation, depending on its temperature T [K], emission coefficient ϵ [-] and the Stefan-Boltzmann constant σ [W/m^2K]. The resulting radiation P/A [W/m^2] emitted by an object can be calculated using the Stefan-Boltzmann Law in Equation 2.3 [8].

$$\frac{P}{A} = \epsilon\sigma T^4 \quad (2.3)$$

Section 2.2 will address different heating technologies that use conductive, convective or radiative heat transfer to heat residential buildings.

2.2 RESIDENTIAL HEATING TECHNOLOGIES

According to the Second Law of Thermodynamics, it is physically impossible to transport heat from a low-temperature area to a high-temperature area without

adding additional energy to the system. Numerous heating techniques are available that use this principle, such as the traditional boiler heating system that runs on fossil fuels. The Section starts by explaining the operation of a gas boiler. Afterwards, this Section considers several alternative technologies that would be more appropriate choices in a modernised low-carbon or zero-energy building. These technologies are heat pumps, infrared panels and photovoltaic thermal collectors. The Section will be concluded by comparing the different technologies. Since the scope of this research is limited to the heating system of a Dutch residence, cooling technologies are not considered due to the Dutch mild maritime climate.

2.2.1 Gas Boiler

A traditional gas boiler, currently implemented in most Dutch households, consists of a furnace, heat exchanger, electric pump and a flue. When installed in a home, it is connected to a thermostat. The gas boiler will switch on when the measured temperature by the thermostat drops below the temperature set by the user, for instance, 20 °C. The gas valve will open to supply gas to the furnace, where the gas is burned, and the majority of the generated heat is transferred to the water by a heat exchanger. A pump then distributes the heated water through the installed radiators. Finally, the byproducts formed during combustion leave the furnace through a flue. [10]. An overview of the mentioned components in a gas boiler can be seen in Figure 2.1. For every m³ of natural gas burned, 1.8 kg of CO₂ is emitted.

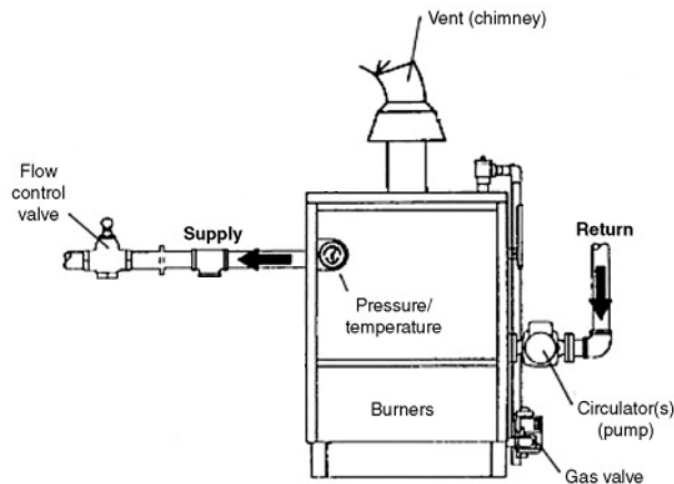


Figure 2.1: The components of a gas boiler. Adapted from [11].

A natural gas boiler has a specific efficiency η_{boiler} , which can be calculated by dividing the delivered heat Q_{output} by the consumed chemical energy E_{input} in the natural gas, as shown in Equation 2.4.

$$\eta_{\text{boiler}} = \frac{Q_{\text{output}}}{E_{\text{input}}} \quad (2.4)$$

2.2.2 Heat Pump

This Subsection describes the operation of a heat pump, as well as the advantages and disadvantages of its implementation. There are heat pumps with both a heating

and cooling mode, and heat pumps with a heating mode only, the latter being more appropriate for this project's scope. A heat pump in heating mode extracts an amount of heat from a low-temperature area, demanding an input of work. This heat is then delivered to a high-temperature area [12, 13].

The most common heat pump types in residential use are air-to-water heat pumps, which transfer heat from ambient air to water. Next to this type, other possibilities are air-to-air heat pumps or geothermal heat pumps. An air-to-air heat pump transfers heat from the air in one area to the air in another area, while geothermal heat pumps exchange heat with the ground, benefiting from its relatively constant temperature.

The traditional residential heating system infrastructure differs from the infrastructure needed for installing heat pumps, as described in Section 2.6. Therefore challenges to implementing heat pumps are initial costs, system design and integration into existing residential buildings. Besides, there are few significant refrigeration enterprises products that sell large-scale heat pumps [12]. Also, the implementation of heat pumps could have adverse economic and environmental effects in countries where fossil fuel-based technologies are still dominant in the national energy mix [14]. Nevertheless, of the heating technologies applicable in net-zero energy buildings, heat pumps are currently the technology with the highest technical maturity, presenting longer lifetimes and less required maintenance than conventional boilers [15].

A heat pump has four main components: an evaporator, a compressor, a condenser and an expansion valve, as illustrated in Figure 2.2a. These components are linked by pipes, through which a refrigerant with appropriate physical properties is flowing.

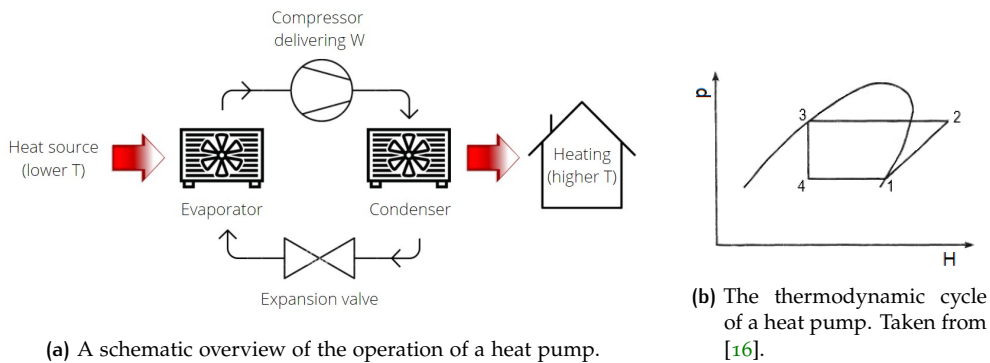


Figure 2.2: Heat pump principles.

At the evaporator, the temperature of the refrigerant is lower than the outside temperature, causing heat transfer to the evaporator, and resulting in evaporation of the refrigerant (step 1). This vapour is then compressed by the compressor, increasing the pressure. This compression takes work, defined by W , and causes the refrigerant to condensate and its temperature to rise (step 2). The ideal gas law in Equation 2.5 explains the temperature rise resulting from the pressure increase:

$$pV = nRT \quad (2.5)$$

The refrigerant temperature is now higher than the indoor temperature, causing heat transfer from the condenser to the air blowing or the water flowing (step 3). Subsequently, the refrigerant flows through the expansion valve, expanding the liquid refrigerant to the evaporating pressure (step 4) and concluding the cycle [16]. An overview of the operation and the thermodynamic cycle can be seen in Figure 2.2. The corresponding stages are numbered and correspond with the numbers in the text.

Coefficient of Performance

The Coefficient of Performance (COP) of a heating technology is defined as the ratio of supplied heat to the work input and is shown in Equation 2.6. For a heat pump, the maximum theoretical COP depends on the outdoor and indoor temperatures T_{out} and T_{in} [13, 16].

$$\text{COP} = \frac{Q_{\text{output}}}{W_{\text{input}}} \quad (2.6)$$

$$\text{COP}_{\text{HP}}^{\text{max}} = \frac{T_{\text{in}}}{T_{\text{in}} - T_{\text{out}}} \quad (2.7)$$

Equation 2.7 shows that the COP decreases for lower outdoor temperatures T_{out} , assuming that the indoor temperature T_{in} remains relatively constant at around 20 °C. In reality, the COP of heat pumps is lower than the $\text{COP}_{\text{HP}}^{\text{max}}$ that can be calculated from Equation 2.7.

Other relevant parameters that describe the energy performance of heat pumps are the Seasonal Coefficient of Performance (SCOP) and the Seasonal Performance Factor (SPF), enabling them to deal with the fluctuating COP. The SCOP describes the average COP during a heating season. The SPF is the net seasonal COP in active mode, defined as the ratio between the annual energy provided by the heat pump and the annual energy supplied to the heat pump [17].

Working Fluids for Heat Pumps

As mentioned before, a heat pump works with a working fluid called a refrigerant. Several optional fluids and their physical properties are listed in Table 2.1.

For a refrigerant to be suitable for a residential heat pump, its thermodynamic properties should be such that the freezing risk of the fluid is minimised. Therefore the freezing point at the operating pressure should be sufficiently below temperatures that occur in Dutch weather conditions. Furthermore, the critical temperature should be higher than the desired indoor temperature to ensure that the working fluid can be liquefied. Additionally, the boiling point at the operating pressure should lie between the indoor and outdoor temperature. Finally, a low specific volume is desired to compact the heat pump components.

Table 2.1: Several available refrigerants [18]. The boiling and freezing point are given at p_{atm} and can be increased by applying higher operating pressure.

Refrigerant no.	Name	Molecular Mass (g/mol)	Boiling Point (°C)	Freezing Point (°C)	Critical Temperature (°C)	Critical Pressure (bar)	Specific Volume (m ³ /kg)
R-11	Trichlorofluoromethane ¹)	137.37	23.8	-111	198	44.1	554
R-12	Dichlorodifluoromethane ²)	120.91	-29.9	-158	112	41.2	558
R-13	Monochlorotrifluoromethane	104.46	-81.4	-181	29	38.7	578
R-13B1	Bromotrifluoromethane	148.91	-57.8	-168	67	39.6	745
R-14	Tetrafluoromethane (Carbon tetrafluoride)	88.00	-128.0	-184	-46	37.4	626
R-22	Difluoromonochloromethane ³)	86.47	-40.7	-160	96	49.8	525
R-40	Chloromethane (Methyl Chloride)	50.49	-23.7	-98	143	66.8	353
R-113	Trichlorotrifluoroethane ⁴)	187.39	47.8	-35	214	34.4	576
R-114	1,2-dichloro-1,1,2,2-tetrafluoroethane	170.92	3.6	-94	146	32.6	582
R-115	Chloropentafluoroethane	154.47	-38.9	-101	80	31.6	614
R-134a	Tetrafluoroethane ⁶)	102.03	-26.1	-97	101	40.7	552
R-142b	1-chloro-1,1-difluoroethane	100.50	-10.0	-131	137	41.2	435
R-170	Ethane	30.07	-88.3	-172	32	49.0	193
R-290	Propane	44.10	-42.2	-190	97	42.5	220
RC-318	Octafluorocyclobutane	200.04	-5.6	-42	116	27.9	621
R-500	Dichlorodifluoromethane/	99.31	-33.3	-159	106	44.3	496
R-600	n-Butane	58.12	-0.4	-138	152	38.0	228
R-600a	Isobutane (2-Methyl propane)	58.12	-11.8	-145	135	36.5	221
R-611	Methyl formate	60.05	31.7	-99	214	60.0	349
R-717	Ammonia	17.02	-33.3	-78	133	114.2	236
R-744	Carbon Dioxide	44.01	-78.6	-57	31	73.8	468
R-764	Sulfur Dioxide	64.06	-10.0	-76	158	78.8	523
R-1150	Ethylene	28.05	-104.0	-169	9	51.2	229
R-1270	Propylene	42.08	-47.8	-185	92	46.2	222

2.2.3 Photovoltaic Thermal Modules

Photovoltaic Thermal (PVT) collectors combine the technologies of photovoltaic modules and solar thermal collectors into a single device, producing both electrical and thermal energy. This combination results in a higher efficiency compared to traditional Photovoltaic (PV) panels [19].

Electromagnetic radiation from the sun consists of photons propagating with a particular wavelength. The energy of each photon can be related to its wavelength according to Equation 2.8, also known as the Planck-Einstein relation.

$$E_{\text{ph}} = \frac{hc}{\lambda} \quad (2.8)$$

This energy can be converted into either electrical or thermal energy. Electrical energy is generated using PV cells, generally made of silicon. The bandgap energy E_G of crystalline silicon is 1.12 eV. Photons with an energy E_{ph} higher than the bandgap energy can excite electrons to a higher state and create electron-hole pairs. This process leads to an electric field, driving current generation, and therefore, electricity.

Photons with an energy lower than 1.12 eV cannot excite electrons and can therefore not convert their energy into electricity. In addition, photons with an energy higher than 1.12 eV do not use their full energy potential; the remaining energy is released as heat. These two factors combined are known as spectral mismatch, illustrated in Figure 2.3.

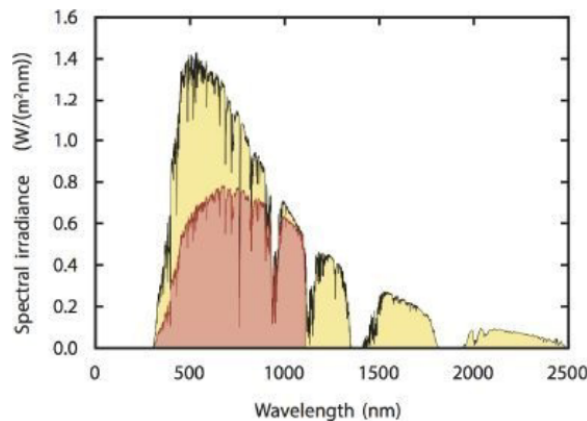


Figure 2.3: The fraction (in red) of the solar spectrum (in yellow) that can be converted into electrical energy by a c-Si solar cell. Taken from [9].

In Figure 2.3, the total solar spectrum is displayed in yellow. It represents the amount of sunlight, in $W/(m^2nm)$, that reaches the surface of the earth at Standard Test Conditions (STC). The convertible fraction of the solar spectrum is displayed in red. This fraction is known as the Shockley-Queisser limit.

A PVT module, however, avoids this spectral mismatch because the heat released by high energy photons can be absorbed, and the energy of low energy photons can be converted into thermal energy. In contrast to a traditional PV module, a solar thermal collector can generate energy from the entire solar spectrum.

Furthermore, PVT collectors have a higher lifetime than traditional PV systems since the solar thermal collector will prevent damage to the photovoltaic cells due to high temperatures by absorbing and carrying away the generated heat [20]. Increasing the cooling of the photovoltaic cell can be done by increasing the mass flow rate of water through the thermal collector.

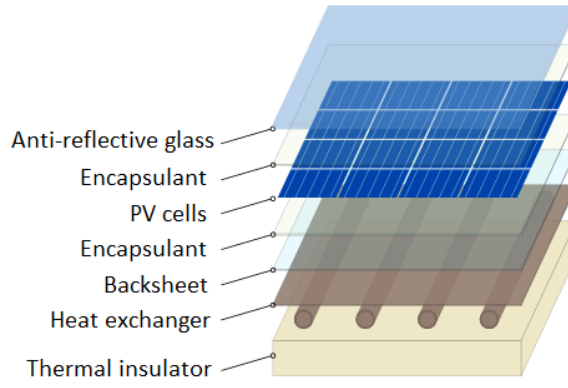


Figure 2.4: The components of a PVT collector. Taken from [21].

An overview of a PVT collector can be seen in Figure 2.4, and it consists of different layers. The PV cell layer is protected by an encapsulant, and the amount of reflected sunlight is reduced by an anti-reflective layer. Behind the PV cell layer, there is a heat exchanger and a layer of thermal insulation to enhance the thermal energy yield and prevent heat loss.

First of all, incident sunlight passes through the PV cells, where a part of the sunlight is absorbed. During this process, the excess energy of the photons is released as heat. The generated heat Q_{PV}^{thermal} is then transferred by conduction to the thermal absorber, situated behind the PV cells. The second way in which thermal energy can be generated is by photons that were transmitted by the PV cell. These transmitted photons can transfer their energy to the thermal absorber by radiation. The potential transferred radiative heat is the energy provided by the sun E_{sun} , minus the potential radiative heat from the photons absorbed by the photovoltaic cell, Q_{PV}^{abs} .

It is vital to maintain a lower operating temperature for thermal energy in the absorber, collected by these two processes, is then transferred to the liquid in the tube network by conduction. Finally, the thermal energy is carried to the heating system through isolated pipes, an example of convective heat transfer. The overall efficiency of a PVT module η_{PVT} can be calculated using Equation 2.9.

$$\eta_{PVT} = \eta_{PV} + \eta_T = \frac{E_{\text{electric}} + Q_{\text{gen}}}{E_{\text{sun}}} \quad (2.9)$$

Fudholi et al. [20] determined the performance of PVT collectors and found an overall efficiency of around 65%, with an electrical efficiency of 13% and a thermal efficiency of 52%. This efficiency is the result of several energy losses in a PVT panel. There is convective heat loss Q_{conv} from the PVT panel to the ambient and radiation Q_{rad} from the thermal absorber to the ambient. Moreover, there are losses resulting from the reflection of photons Q_{refl} , by either the photovoltaic cell or thermal absorber, incomplete absorption of photons and recombination losses in the photovoltaic cell. These losses can be combined in the heat balance in Equation 2.10.

$$Q_{\text{gen}} = E_{\text{sun}} - Q_{PV}^{\text{abs}} + Q_{PV}^{\text{thermal}} - Q_{\text{refl}} - Q_{\text{rad}} - Q_{\text{conv}} \quad (2.10)$$

When the operating temperature increases, the electrical yield of a PV cell decreases. Therefore, the operating temperature of PVT systems is limited by PV cells [22]. PVT cannot be used as a heating technology on its own since the temperatures of the working fluid will not reach the temperature required for space heating. Single solar thermal collectors can reach higher temperatures than PVT collectors because the operating temperature of PV cells does not limit them.

The thermal efficiency of PVT collectors can be increased by adding a glass layer on top of the solar cells, though this comes at the cost of electrical efficiency [23]. In

summer, when heating demand is low whereas thermal energy yield is high, excess energy generated by PVT collectors could be stored if Thermal Energy Storage (TES) is added to the system, see Section 2.3.

Current challenges and future research subjects for PVT modules involve the structural module design and selecting an appropriate working fluid that is both economically and environmentally advantageous [24] to minimise module cost and maximise environmental benefits.

2.2.4 Infrared Panels

Infrared heating technology is based on radiant heat transfer. Radiation implies that in a room with infrared panels, most heat is transferred to solid objects, such as furniture, walls and humans, whereas the air temperature in a room is nearly not affected by infrared heating [25]; this is illustrated in Figure 2.5b. A benefit of this is that the heat transfer is more efficient since the heat is transferred directly to the object, without the air as an intermediate carrier.

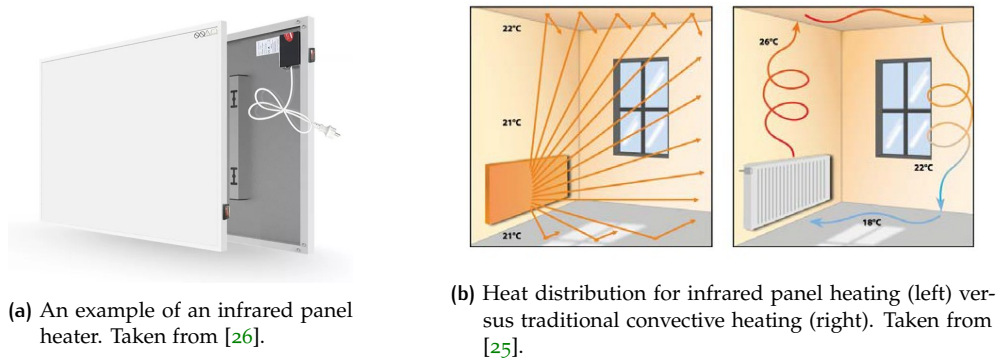


Figure 2.5: Infrared panel heating.

This technology is relatively new, and therefore, little is known about its exact efficiency. Furthermore, it is challenging to compare the COP of infrared heaters to the COP of other technologies since radiant heating requires less energy than convective heating technologies for the same amount of comfort.

2.2.5 Comparison of Heating Technologies

An overview is presented in Table 2.2 to compare the previously mentioned heating technologies, listing the most important properties of each technology. The costs are split into capital, maintenance and incremental costs.

Table 2.2: A comparing table on different heating technologies.

	Gas boiler	Heat pump	Infrared ¹	PVT ²
COP	0.93	3.0-4.0	0.8-1.0	0.35-0.65
Costs: capital (€/kW)	170	600	75-110	3000
Costs: maintenance (€/year)	70	100	0	10
Costs: incremental (€/kWh)	0.11	0.05	0.18	0
Lifetime (years)	15	18	30	30
Environmental impact ³	High	Low	Low	Low

¹ Radiant heating requires a lower amount of energy for the same amount of comfort.

² PVT panels cannot cover the total heating demand due to the maximum reachable temperature of the working fluid.

³ The environmental impact of heat pumps and infrared heaters was determined assuming renewable electricity consumption.

Based on Table 2.2 and the average heating demand, it is possible to calculate the Levelised Cost of Energy (LCOE), a tool that allows comparing the average cost of different heating technologies over their lifetime. This calculation can be carried out by using Equation 2.11.

$$\text{LCOE} = \frac{\sum_{t=1}^n \frac{I_t + M_t + F_t}{(1+r)^t}}{\sum_{t=1}^n \frac{E_t}{(1+r)^t}} \quad (2.11)$$

In this Equation, I_t are the capital costs in year t , M_t are the operational and maintenance costs in year t , and F_t are the fuel costs in year t . E_t is the energy generated in year t , and n is the expected lifetime of the technology. r is the discount rate, which is the yearly interest rate to be obtained if the capital was invested in interest-bearing assets instead.

For the calculations, an average heating demand of 9550 kWh [27] and a discount rate of 6% was assumed. Furthermore, the gas and electricity prices were considered to be stable. The generated electrical energy was also taken into account for the PVT system. The results can be seen in Table 2.3 below.

Table 2.3: The calculated LCOE of different heating technologies.

	Gas boiler	Heat pump	Infrared	PVT
LCOE (€/kWh)	0.16	0.11	0.19	0.17

Marinelle et al. stated that “if the COP of the heat pump is above 3, the heat pump heating system has a high economic and environmental integrated performance, i.e. a lower cost and less environmental impact than the other systems investigated (coal and gas boiler)” [28]. This statement is confirmed by the results from Table 2.3, where the LCOE of the heat pump was calculated using a COP of 3.

2.3 THERMAL ENERGY STORAGE

The transition to renewable energy sources will involve more fluctuations in power generation, resulting in the need for large-scale energy storage technologies [29, 3, 4, 30, 31]. Sensible TES, for example, is 50-100 times cheaper than electrical energy storage [32, 33]. Additionally, TES can be suitable for both short-term and long-term storage applications, making TES an excellent storage option to improve the flexibility of the electrical grid, for example, by shaving heat demand peaks [34].

This Section starts with a general explanation of TES and its different types, followed by Section 2.3.2 on thermal energy storage tanks.

2.3.1 Types of Thermal Energy Storage

TES is a technology that saves thermal energy to use at a later moment by heating or cooling a material. The stocked energy can be used at another time for heating, cooling or power generation [35]. There are three different types of TES: sensible, latent and thermochemical. Sensible Heat Storage (SHS) stores energy by temperature changes in a medium. Latent Heat Storage (LHS) uses the energy released or taken up by phase changes, and Thermochemical Heat Storage (THS) uses the energy related to reversible chemical reactions. SHS is currently the most mature technology [36]. While LHS has a higher potential capacity and a more constant heat release temperature, its application is limited due to poor heat transfer, significant heat losses and super-cooling [24]. THS is a promising method with the benefits of high energy density, low heat losses and good storage operation repeatability. However, this technology is still in the lab stage [37]. The main focus areas for research on TES are the cost reduction of storage material, increasing energy storage efficiency, and improving thermal conductivity [24].

Several technologies that utilise SHS are Tank Thermal Energy Storage (TTES), Pit Thermal Energy Storage (PTES), Aquifer Thermal Energy Storage (ATES) and Borehole Thermal Energy Storage (BTES). These technologies all store thermal energy underground, using the favourable insulating properties of the earth [36]. TTES is most suitable for residential use because of its possibility to apply at a small scale and low impact on the living environment.

2.3.2 Thermal Energy Storage Tanks

A thermal storage tank can be made of concrete, steel or fibre-reinforced plastics and uses water as a storage medium [38]. An example of such a tank used for this project is shown in Chapter 3. Higher storage volumes of the tank lead to lower thermal losses [36]. The stored sensible thermal energy Q_{stored} (J) in a storage tank can be calculated according to Equation 2.12.

$$Q_{stored} = mc_V \Delta T \quad (2.12)$$

In this Equation, m is the mass in kg, c_V is the specific heat capacity of the storage medium in J/(kgK), and ΔT is the temperature difference in K between the initial and current temperature of the medium [9].

Thermal stratification is a phenomenon that can occur in TTES, which is described as the formation of different temperature layers within the storage medium. Since cold water has a higher density, it sinks to the bottom, forming a cold, thermocline and hot region. This phenomenon is illustrated in Figure 2.6 and influences the storage performance [39]. The thermocline layer should be as narrow as possible for higher performance, enabling a greater hot water volume to be stored.

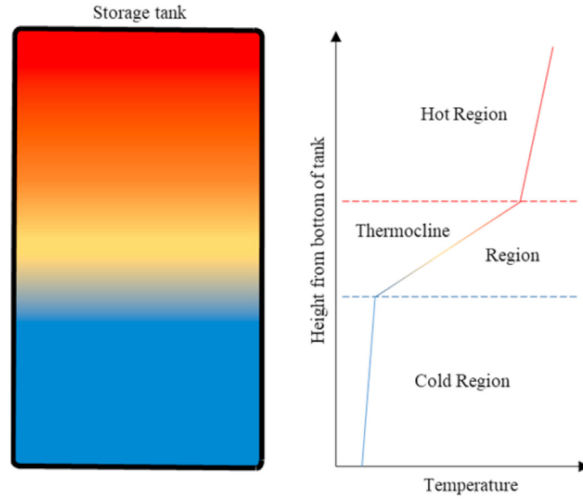


Figure 2.6: Thermal stratification in a storage tank, separating water into different thermal regions: hot, thermocline and cold. Taken from [36].

2.4 THERMAL ENERGY DISTRIBUTION

Once thermal energy is generated, for example by using one of the technologies from Section 2.2, the energy can be distributed through a residential building by pipes and valves. This Section describes the energy flows and losses during the distribution process and considers pipes, valves and heat pipes.

2.4.1 Pipes

A thermal liquid flowing through a pipe is subject to viscous friction losses and convective heat transfer with the pipe wall. Viscous friction losses result in a decrease in pipe pressure, while convective heat transfer changes the temperature of the thermal liquid in the pipe. The direction of heat transfer depends on the liquid and ambient temperatures, where heat is transferred from a high to a low-temperature area.

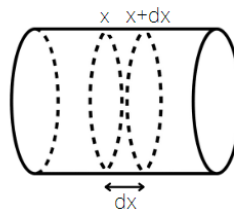


Figure 2.7: An infinitesimal section of a pipe.

The energy balance of an infinitesimal element of a pipe, represented schematically in Figure 2.7, is shown in Equation 2.13 and 2.14 [8]. In this energy balance, it is assumed that the liquid flows in the positive x -direction (from left to right).

$$Q_x^{\text{in}} - Q_{x+dx}^{\text{out}} - Q^{\text{loss}} = 0 \quad (2.13)$$

$$\frac{\pi}{4} D^2 \rho \langle v \rangle [c_p \langle T \rangle]_x - \frac{\pi}{4} D^2 \rho \langle v \rangle [c_p \langle T \rangle]_{x+dx} - h \pi D dx (\langle T \rangle_x - T_w) = 0 \quad (2.14)$$

In this energy balance, D is the inner diameter of the pipe in m, ρ is the density of the liquid in kg/m^3 , $\langle v \rangle$ is the average flow rate of the liquid in m/s, and c_p is the heat capacity in J/kgK. Furthermore, T is the temperature of the liquid in K at cross-

section x or $x + dx$, T_w is the temperature of the pipe wall in K, and h is the heat transfer coefficient in W/m^2K . Equation 2.14 can be rewritten into Equation 2.15.

$$\frac{dT}{dx} = \frac{4h(T_w - T)}{D\rho c_p \langle v \rangle} \quad (2.15)$$

The heat transfer coefficient h can be calculated by Equation 2.16, assuming the Nusselt correlation for turbulent tube flow.

$$h = Nu \frac{\lambda}{D} = 0.027 \frac{\lambda}{D} Re^{0.8} Pr^{0.33} \quad (2.16)$$

In this Equation, λ is the thermal conductivity of the fluid in W/mK . The dimensionless numbers Reynolds and Prandtl in Equation 2.18 are used to demonstrate turbulent flow if their values satisfy the conditions in Equation 2.18.

$$Re = \frac{\rho v D}{\mu} > 10^4 \quad (2.17)$$

$$Pr = \frac{v \rho c_p}{\lambda} \geq 0.7 \quad (2.18)$$

Here μ is the dynamic viscosity in $Pa \cdot s$, and v is the kinematic viscosity in m^2/s . Equation 2.15 - 2.18 can be combined to determine heat loss. Furthermore, the pressure drop ΔP in Pa due to friction can be determined through the Fanning pressure drop equation for turbulent flow in smooth-walled tubes in Equation 2.19. This Equation holds if the Reynolds number satisfies the condition $4000 < Re < 10^5$.

$$\Delta P = 0.316 Re^{-\frac{1}{4}} \frac{L}{D} \frac{1}{2} \rho \langle v \rangle^2 \quad (2.19)$$

2.4.2 Valves

Valves are used to regulate the direction and magnitude of the flow. There are different valve types, such as check valves, gate valves and pressure control valves. Different valve types and their operation are shown in Figure 2.8.

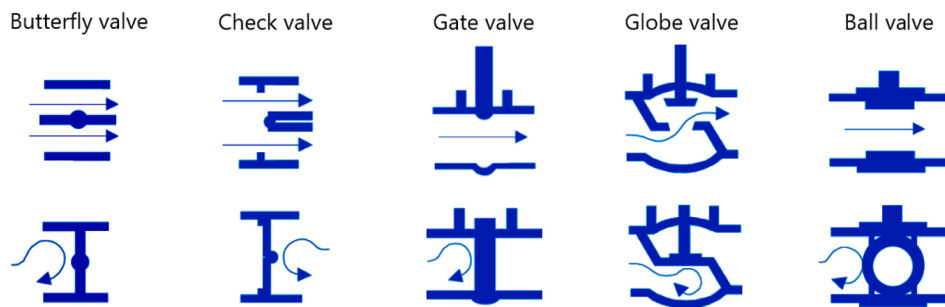


Figure 2.8: Different valve types. Adapted from [40].

It is possible to calculate the pressure drop across a valve using the relation in Equation 2.20.

$$\Delta P = K_w \frac{1}{2} \rho \langle v \rangle^2 \quad (2.20)$$

In this Equation, K_w is a dimensionless coefficient, dependent on the valve type and the degree to which the valve is opened or closed. Values for K_w can be found in literature and datasheets.

2.4.3 Heat Pipes

In contrast to a traditional thermal energy distribution system consisting of tubes and valves, heat pipes are an example of a more innovative technology to distribute thermal energy. Heat pipes occur in an extensive range of sizes and applications and are suitable for integration within, for example, solar collectors and a house heating system [41]. In essence, a heat pipe is an isolated cylindrical thermal energy transport system consisting of an evaporator section, condenser section, and a wick mounted to the inside surface of the cylinder [42]. An overview of this structure can be seen in Figure 2.9. The cylinder is filled with a working fluid with suitable thermodynamic properties, such as boiling temperature.

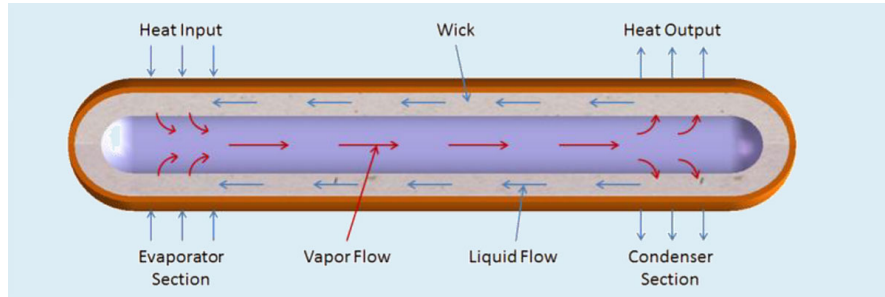


Figure 2.9: A schematic overview of a heat pipe. Taken from [43].

The evaporator section is located at a heat source, such as a solar thermal collector or thermal energy storage device. The condenser section acts as a heat sink, delivering heat to the indoor environment. In the evaporator section, the working fluid absorbs thermal energy and evaporates. The vapour formed flows through the adiabatic section of the heat pipe until it reaches the condenser section, where thermal energy is transferred out of the heat pipe, decreasing the temperature of the working fluid below the boiling point. The condensed liquid flows back to the evaporator section through the wick, closing the cycle [44]. The boiling temperature of the working fluid is such that the fluid evaporates at the evaporator section and condensates at the condensing section.

The physical orientation or flow circuit of combined heat pipes can look like a serpentine circuit, collector circuit or circuit with separate heat pipes [45]. Furthermore, the orientation of heat pipes is not necessarily horizontal or vertical; they can also be mounted at an angle.

Heat pipes do not require an input of work, but they need to be combined with an external heat source. Due to the closed pipe system, this technology is low-maintenance.

2.5 THERMAL LOSSES IN A RESIDENTIAL BUILDING

Thermal losses in residential buildings occur through surfaces such as walls, windows and roofs. The thermal loss through a surface can be calculated with Equation 2.21.

$$\frac{dQ}{dt} = U A \Delta T \quad (2.21)$$

In this Equation, $\frac{dQ}{dt}$ is the heat transfer in W, U is the overall heat transfer coefficient in W/m^2K , A is the surface area in m^2 and ΔT is the temperature difference in $^{\circ}C$. Lastly, the overall heat transfer coefficient U (W/m^2) can be calculated using Equation 2.22.

$$\frac{1}{U} = \frac{1}{h_1} + \sum_{n=1}^N \frac{L_n}{\lambda_n} + \frac{1}{h_2} \quad (2.22)$$

Here, h_1 and h_2 are convective heat transfer coefficients in $\text{W}/\text{m}^2\text{K}$, L is the thickness of the n^{th} layer in m, λ is the thermal conductivity of the n^{th} layer material in W/mK , and N is the total amount of layers. The first and third terms represent thermal resistance through convective heat transfer, and the middle term represents the thermal resistance of the different layers through conductive heat transfer.

These variables are pictured schematically in Figure 2.10. In this figure, heat transfers through a plate from an area with temperature T_1 to an area with temperature T_6 , where $T_1 > T_6$.

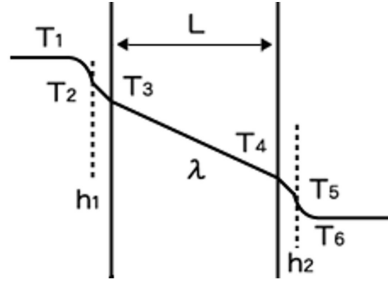


Figure 2.10: A schematic overview of the different components playing a role in heat transfer through a flat plate such as a wall or window.

2.6 HEATING ELECTRIFICATION EFFECTS ON HOUSE POWER NETWORKS

The maximum electric power consumption should be considered when electrifying a heating system. Most residential buildings are equipped with a $3 \times 25\text{A}$ breaker box at 230 V. If, for example, a heat pump with a nominal electric power consumption of 2 kW is installed [46], its maximum power consumption equals approximately 45% of the maximum electrical power consumption. Since this is a significant amount, one should always keep in mind the electrical protections and the existing electrical appliances of a household when designing an electrified heating system.

Schlemminger et al. [47] illustrate this further by showing example daily load curves for a heat pump and an average household without a heat pump. It shows moderate peak loads of about 600 W in homes without a heat pump, while the heat pump load curve reaches values as high as 1600 W in winter.

Moreover, when a heat pump is turned on, there is a peak in the electrical load. This starting peak causes a brief period in which electrical power consumption is elevated above the nominal power consumption. This phenomenon increases the required power capacity even further.

3

METHODOLOGY

This Chapter describes the models used to compare scenarios using different heating technologies. Furthermore, it explains a method to determine the optimal thermal energy buffer capacity that considers payback time and CO₂ emissions.

3.1 HEATING SYSTEM SCENARIOS

Different scenarios of residential heating systems were compared in terms of energy use, costs, and CO₂ emissions. Since most Dutch households are currently heated using a gas boiler, this was used as the reference scenario. In addition, the reference scenario was compared to two other scenarios, a hybrid, and an electrified scenario. An overview of the scenarios can also be seen in Figure 3.1.

- I. **Boiler:** This reference scenario is a system in which a boiler solely heats the household.
- II. **PVT + TESS:** In this scenario, the household is heated by PVT panels and a Thermal Energy Storage System (TESS) is used to buffer the intermittency of the PVT system.
- III. **PVT + TESS + HP:** This scenario adds a Heat Pump (HP) to the previous scenario.

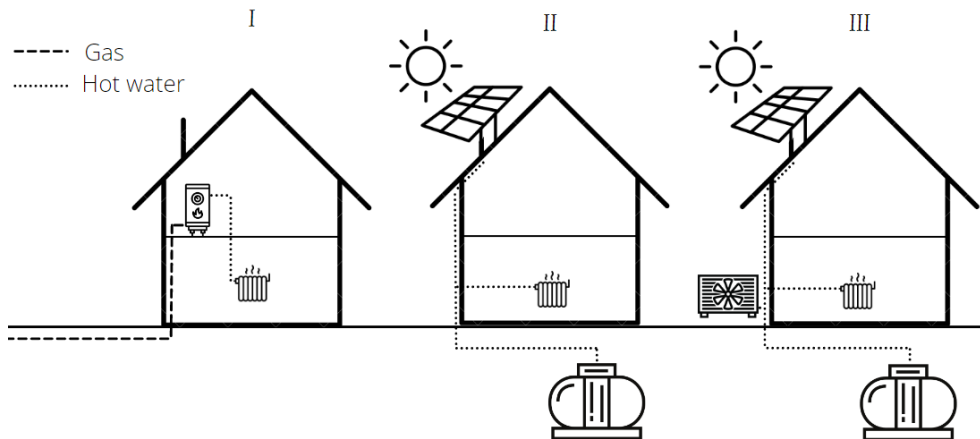


Figure 3.1: A representation of the three different system architectures. From left to right, the systems are (I) a boiler system, (II) a combined PVT and buffer system, and (III) a system with a PVT, buffer and heat pump.

3.2 DATA

Annual data from 2020 was used for outdoor temperature, solar irradiation, and solar inclination. This data was hourly and was obtained from the Royal Dutch Meteorological Institute (KNMI) [48]. Furthermore, a dataset was generated for

indoor setpoint temperature. To create this dataset, it was assumed that the desired indoor temperature is 18 °C from 6 AM until 7 PM and 15 °C at other times.

3.3 MODELS

The scenarios explained in Section 3.1 were modelled using Simscape, a tool from MATLAB & Simulink to simulate multidomain physical systems. This Section describes the models for the house and the different scenarios.

3.3.1 Residential Heating System

Each scenario contains the subsystem shown in Figure 3.2, and it models the heat distribution in a residential building. The modelled house is an average apartment of 120 m², consisting of four rooms and four radiators. It has energy label C, according to Dutch standards [49]. The house is a single floor, and the outdoor walls are assumed to be in contact with the ambient; therefore, heat transfer with neighbouring houses is not considered. Moreover, effects due to wind were not taken into account, and the roof pitch angle is 40 degrees.

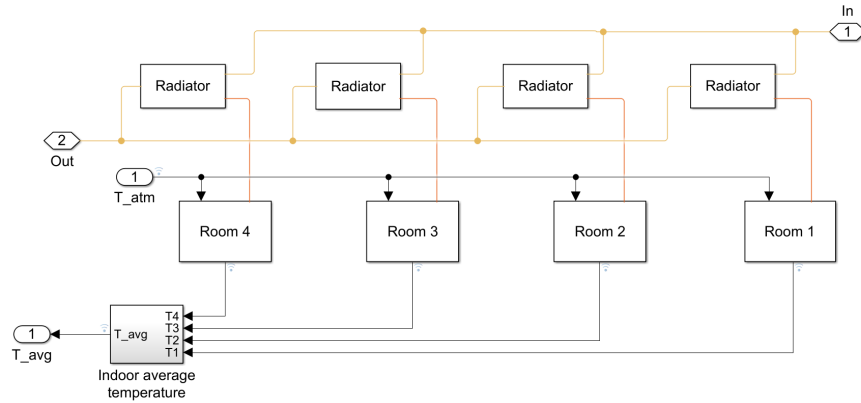


Figure 3.2: The heat flow in a residential building as modelled in Simulink. Yellow lines represent the thermal liquid domain, and orange lines represent the thermal domain.

In the subsystem shown in Figure 3.2, water circulates through the radiators, heating the house provided a thermal energy source added heat. This source varies for each scenario, and its heat transfer is modelled outside the house subsystem. After considering heat gains and losses in each individual room, the average indoor temperature is calculated. The subsystems for the radiators and rooms are shown in Figure 3.3 and 3.4, respectively.

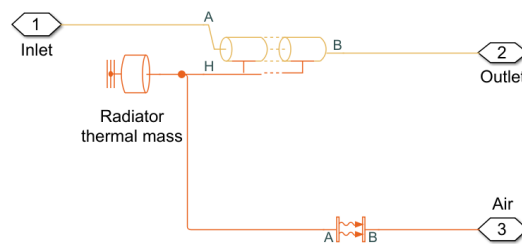


Figure 3.3: The radiator subsystem. Yellow lines represent the thermal liquid domain, and orange lines represent the thermal domain.

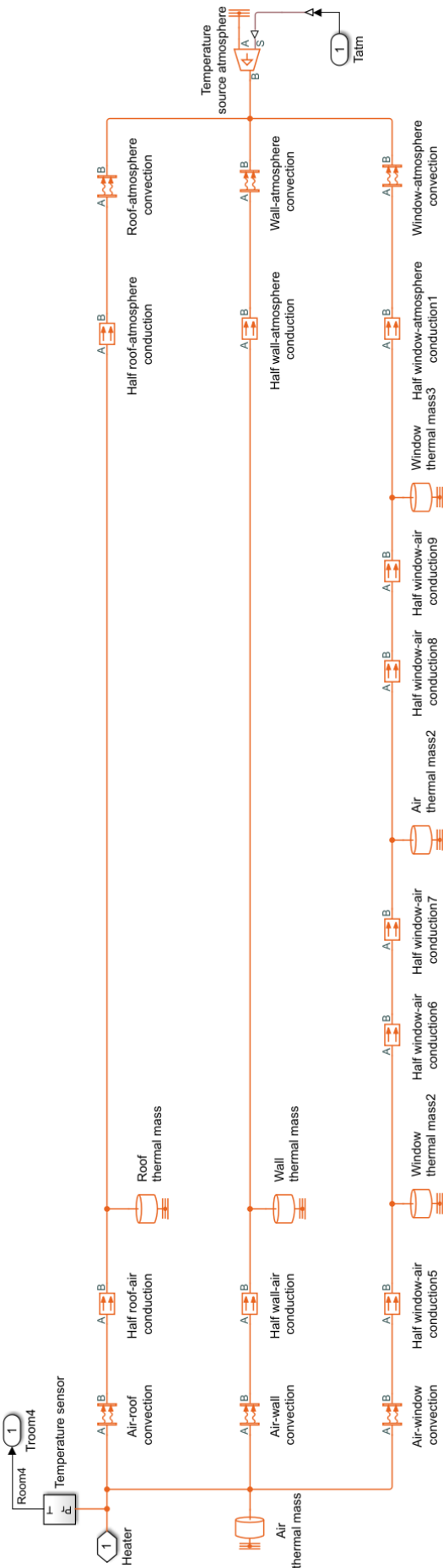


Figure 3.4: The room subsystem contains the thermal losses through walls, roof, and windows.

The radiator subsystem in Figure 3.3 consists of a pipe through which heated water flows from the thermal energy source. This heat is transferred to the thermal mass of the radiator and subsequently to the air in the room by convection.

The room subsystem comprises three parallel strings, representing the heat transfer through the roofs, walls, and windows, respectively. As described in Section 2.5, heat transfer through a flat plate occurs by conduction and convection. Therefore the model consists of different blocks representing these types of heat transfer. The windows are modelled as double-glazed windows, explaining the extra blocks in this string.

All defined parameters, such as dimensions and material properties of the walls, windows, roof, and radiators, can be found in Appendix A. Overall heat transfer coefficients were calculated using Equation 2.22 and compared to values found in literature [49].

3.3.2 Scenario I: Boiler

A draft model from Mathworks was used to create the boiler heating system model [50]. The final model can be seen in Figure 3.5. The model consists of several subsystems: the house, heater, and control system. The control and heater subsystem are shown in Figure 3.6 and 3.7 and clarified in the accompanying text.

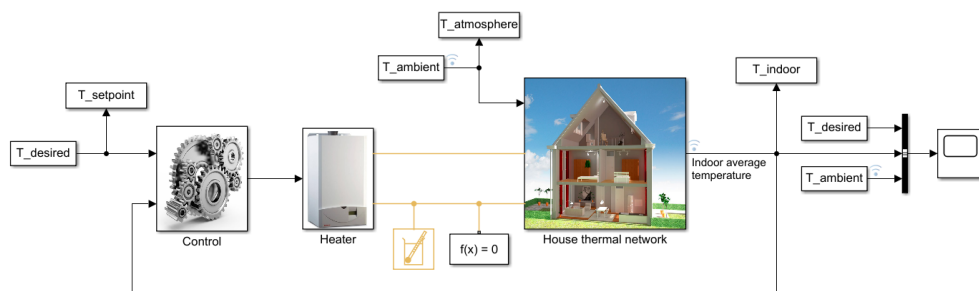


Figure 3.5: This Simulink model simulates a house with a traditional heating system.

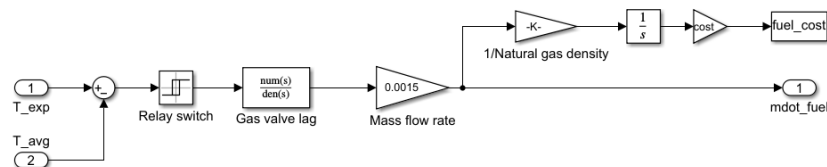


Figure 3.6: The control subsystem.

In the control subsystem in Figure 3.6, the fuel mass flow is switched on when the average indoor temperature reaches a value lower than the setpoint temperature. This subsystem also uses the mass flow to calculate the cost of the consumed fuel, in this case, natural gas.

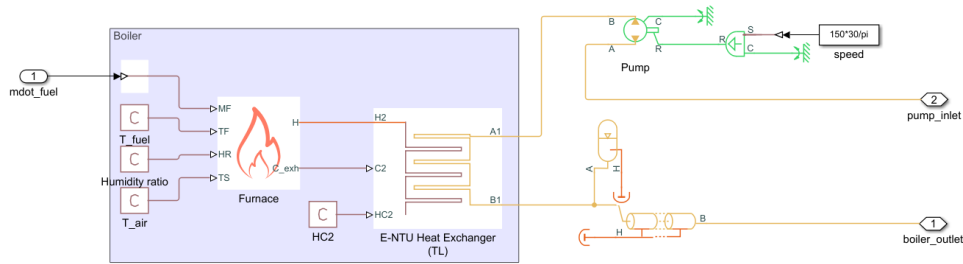


Figure 3.7: The heater subsystem. Yellow lines represent the thermal liquid domain, orange lines represent the thermal domain, and green lines represent the mechanical rotational domain.

The heater subsystem is shown in Figure 3.7; its main components are a furnace, a heat exchanger, and a pump. A mass flow of fuel is provided to the furnace, where the fuel is burned, and heat is generated. The generated heat is transferred to the thermal fluid by a heat exchanger. The thermal fluid is circulated through the radiators in the house by a pump.

3.3.3 Scenario II: PVT + TESS

This Section describes the model used to simulate scenario II. In this scenario, the primary source to satisfy the heat demand is a PVT module, and the secondary source is Borg's thermal energy storage tank. An overview of the model is shown below in Figure 3.8. This model was used to determine the temperature variation inside the house and the tank for different amounts of PVT panels and TESS capacity.

According to the World Health Organization [51], the lowest acceptable indoor temperature is 16 °C. This boundary value was used to determine the number of uncomfortable days in the house for each number of PVT panels and TESS capacity. A Matlab script measured the indoor temperature daily at 5 PM and compared this value to the boundary value. Seventeen cases were modelled in total. The considered PVT sizing was 0, 1, 2 and 3 panels, and the investigated TESS capacity was 0, 2, 4 and 6 m³. Furthermore, a reference case was modelled without any PVT or buffer capacity to determine the number of days that heating was needed.

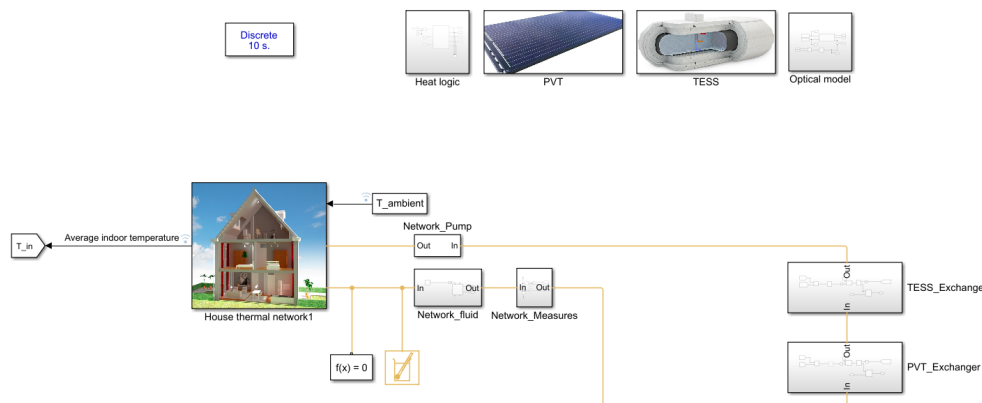


Figure 3.8: This Simulink model simulates a house with a heating system consisting of a PVT system and a TESS.

As seen from Figure 3.8, the Simulink model consists of the house subsystem, a subsystem to add flowing fluid to the network, and two heat exchangers for each of the thermal energy sources. The amount of heat exchanged with the network is

calculated in the subsystems 'PVT' and 'TESS', shown in Figure 3.10 and 3.11 respectively. The computed heat exchange is virtual, i.e. there is no physical connection in the model where thermal energy is transferred from a source to the house.

The logic of the heat exchange is computed in a flowchart, displayed in Figure 3.9. It shows whether the PVT system should be connected and whether the TESS should be charged, discharged or disconnected.

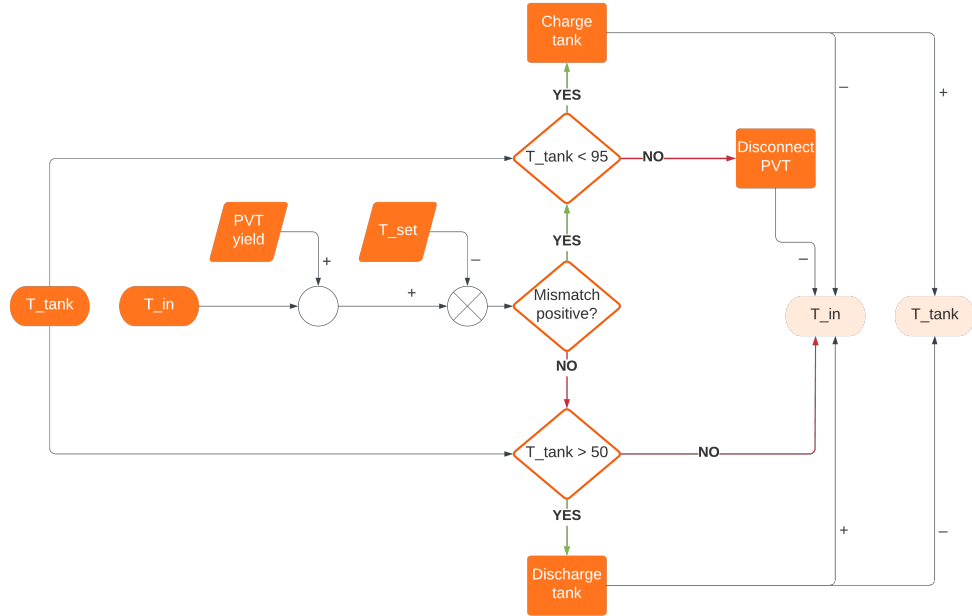


Figure 3.9: A flowchart representing the control strategy of the model.

PVT

The primary thermal energy source in this scenario is a PVT module. The Simulink model that was used to simulate this module was based on a Mathworks draft model [52] and is shown below in Figure 3.10. All relevant parameters of the PVT module can be observed in Appendix E.

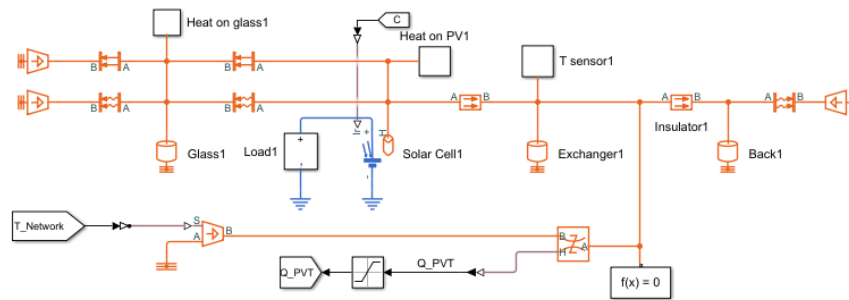


Figure 3.10: The PVT subsystem.

The PVT subsystem models the generated electrical energy as well as the thermal energy; however, only the generated thermal energy was considered in this case. The thermal network models the convective, conductive, and radiative heat transfer between the components of the PVT panel, which are pictured in Figure 2.4.

The inputs of the PVT subsystem are calculated by the optical model subsystem. This subsystem consists of a Matlab function that calculates the transmitted irradiance on the PV cells, the heat absorbed by the glass, and the radiative power

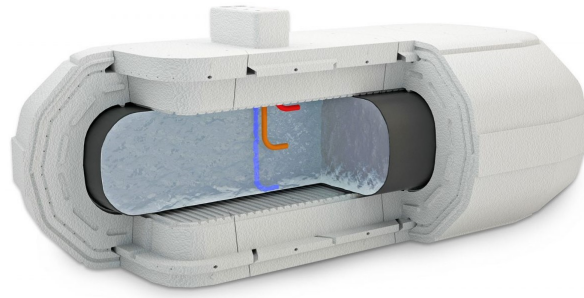


Figure 3.12: The Borg thermal energy storage tank prototype that is installed in The Green Village on the TU Delft campus. Taken from [6].

Payback Time

As mentioned before, a reference scenario was modelled with 0 PVT panels and no buffer capacity. The number of uncomfortable days in this scenario could then be used to determine the yearly avoided natural gas consumption, and thus, the payback time of the system. The payback time can be calculated using Equation 3.1.

$$C_{\text{total}} = -C_{\text{fixed}} + V_{\text{NG,avoided}} \sum_{t=0}^T C_{\text{fuel}} \cdot (1+r)^t \quad (3.1)$$

In this Equation, C_{fixed} are the capital costs in €, $V_{\text{NG,avoided}}$ the yearly avoided gas consumption in m^3 , C_{fuel} is the gas price which is taken to be 0.8 €/m^3 [53]. r is the average increase rate of the gas price in each year t , and is taken to be 0.0157 or 1.57%. C_{total} is the cost balance after T years, and the payback time is the first value of T for which C_{total} is positive. The values that were used to estimate C_{fixed} can be seen from Table 3.2.

Table 3.2: An estimation for the initial costs for PVT modules and a TESS.

Element	Quantity	C_{fixed} (€)
PVT	1 panel	3000
	2 m^3	12000
TESS	4 m^3	15000
	6 m^3	18000

3.3.4 Scenario III: PVT + TESS + HP

In scenario III, the house is heated using PVT modules, a TESS and a HP. This scenario is similar to scenario II; however, a heat pump is added as a tertiary thermal energy source. The Simulink model used to simulate the indoor temperature can be seen in Figure 3.13.

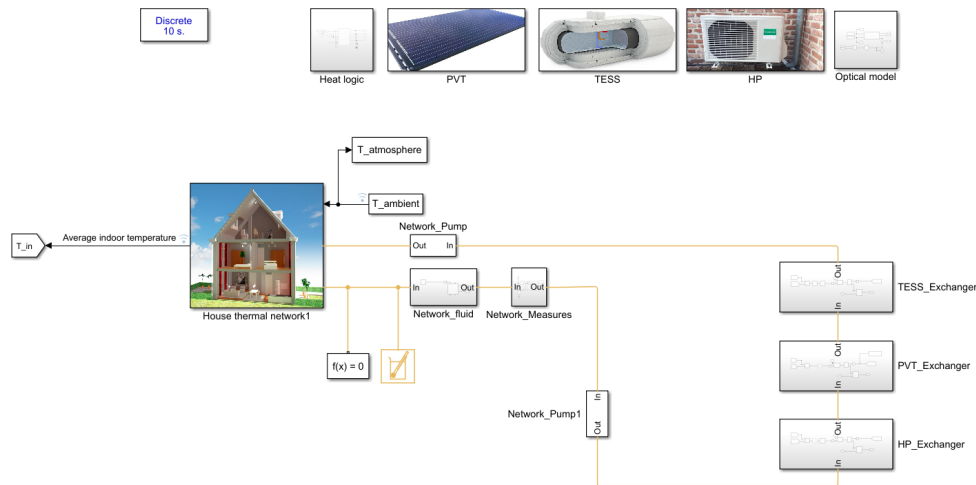


Figure 3.13: This Simulink model simulates a house with a heating system consisting of a PVT system, TESS, and HP.

Heat Pump

The tertiary thermal energy source in this scenario is a heat pump. The heat pump is turned on when the PVT module and TESS do not meet the heat demand. Similar to the method used by Meesenburg et al. [54], the heat pump was modelled as an on/off heat pump with linear ramping rates. The nominal heat output was 2 kW, the ramping-up rate was chosen to be 0.889 W/s, and the ramping-down rate was 0.667 W/s [54]. Figure 3.14 shows a graphical representation of the implemented load curve. An actual load curve has an exponential shape rather than being linear.

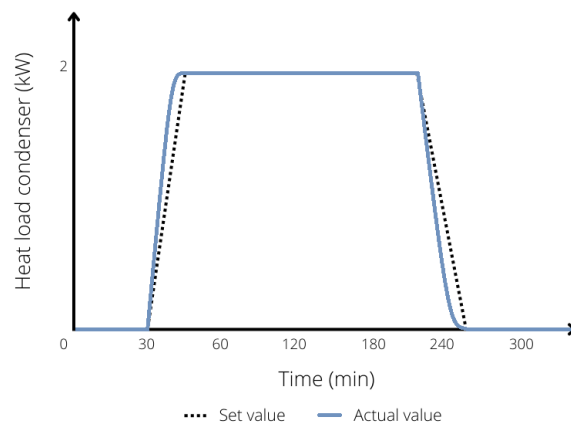


Figure 3.14: The implemented heat pump load curve. The y-axis shows the heat load of the condenser in W, which is the heat output of the heat pump. The x-axis shows the time in minutes.

4 | RESULTS

This Chapter presents the main results obtained in the performed study. First of all, the results of scenario I are covered. Subsequently, the results of scenario II are discussed, and finally, the results of scenario III are presented.

4.1 SCENARIO I: BOILER

This Section contains results for scenario I. Additional results of this scenario can be found in Appendix B. Figure 4.1 shows the yearly variation of the outdoor, indoor, and setpoint temperatures. In warmer months, the house needs less heating, and the daily variation in indoor temperature is lower than in winter. When the boiler is required to heat the home in colder months, the indoor temperature toggles around the setpoint temperature. This effect can be observed more closely in Figure 4.2.

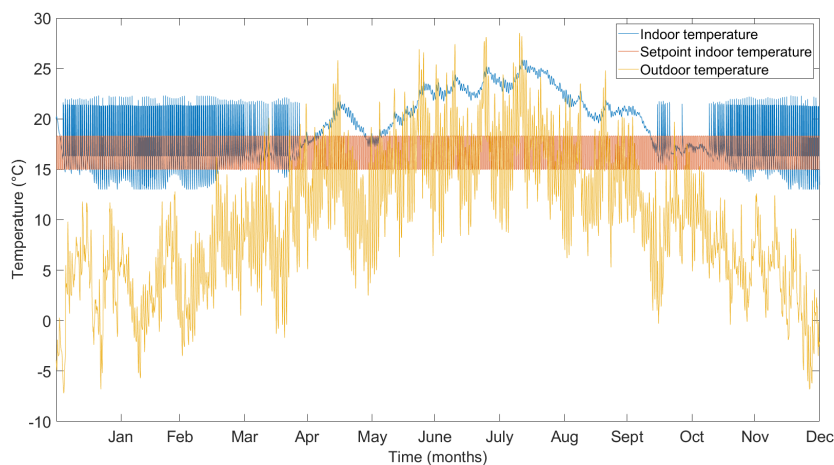


Figure 4.1: Yearly temperature variation in scenario I.

Figure 4.2 shows a zoomed-in version of Figure 4.1, for each of the four seasons. Sharp peaks occur in the indoor temperature when the boiler is activated. Subsequently, the provided heat is transferred to the house's surroundings until the indoor temperature drops below the setpoint temperature and the boiler is activated again. During colder days, the boiler is activated more often. After the boiler turns off, an exponential decrease in indoor temperature is observed. This decrease is expected due to the nature of the differential equations describing heat loss, such as Equation 2.15. Additionally, due to the lower ambient temperature in winter, the indoor temperature drops more quickly once the boiler turns off.

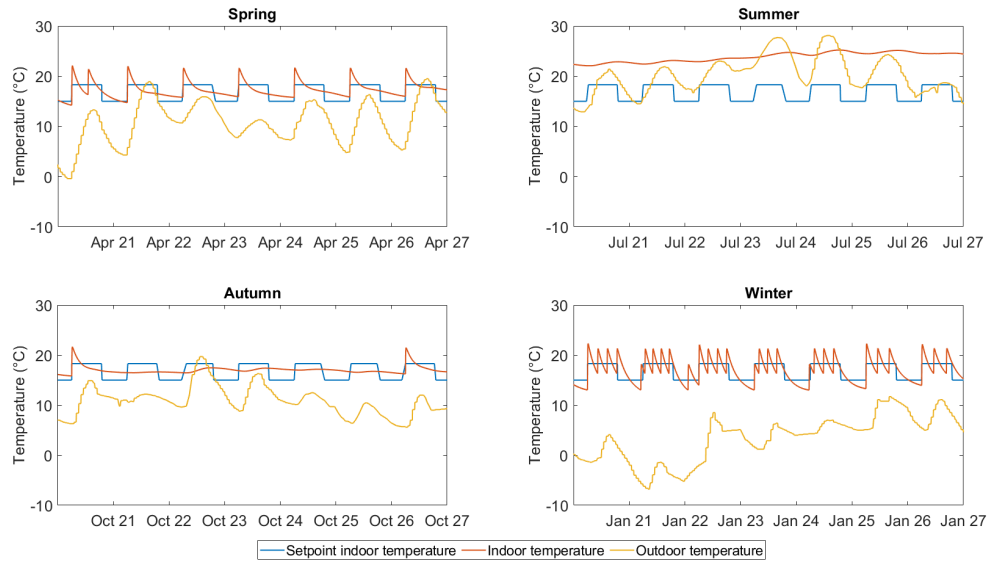


Figure 4.2: Seasonal temperature variation in scenario I.

4.1.1 Fuel Costs

Figure 4.3 shows the cumulative cost of natural gas throughout the year. It can be observed that most fuel is consumed in colder months, as expected. The total yearly heat consumption equals 18.4 GJ or 5109 kWh, and the total volume of gas consumed is 202 m³. At the end of the year, the total cost is €162, assuming a natural gas price of 0.80 €/m³. The total amount of CO₂ emitted is 378 kg.

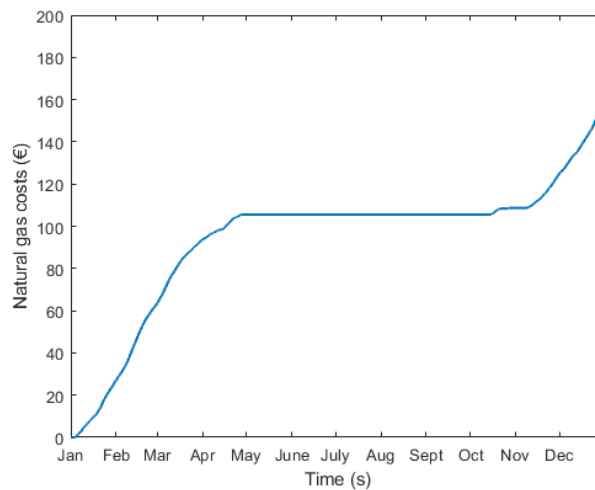


Figure 4.3: The cumulative cost curve for an entire year.

4.2 SCENARIO II: PVT + TESS

This Section presents results for scenario II, in which PVT panels heat the house, and a TESS buffers the intermittency of the PVT system. Figure 4.4 shows the number of uncomfortable days for each system sizing, according to the World Health Organization standards mentioned in Section 3.3.3.

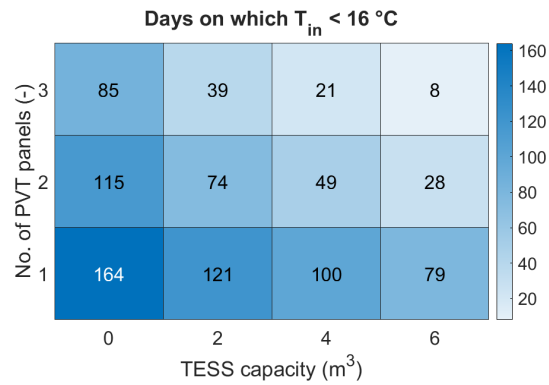


Figure 4.4: The number of uncomfortable days for each system size in a year.

As seen in Figure 4.4, increasing PVT or TESS capacity significantly affects the number of uncomfortable days on which additional heating is needed. Moreover, doubling or tripling the PVT capacity influences the number of uncomfortable days more than doubling or tripling the TESS capacity.

Figure 4.5 and 4.7 show the temperature variation for the system sizing of 1 PVT panel and a buffer capacity of 4 m^3 . In contrast, Figures 4.6 and 4.8 show the temperature variation for the system sizing of 3 PVT panels and a buffer capacity of 6 m^3 . The results of the remaining system sizes can be seen in Appendix C.

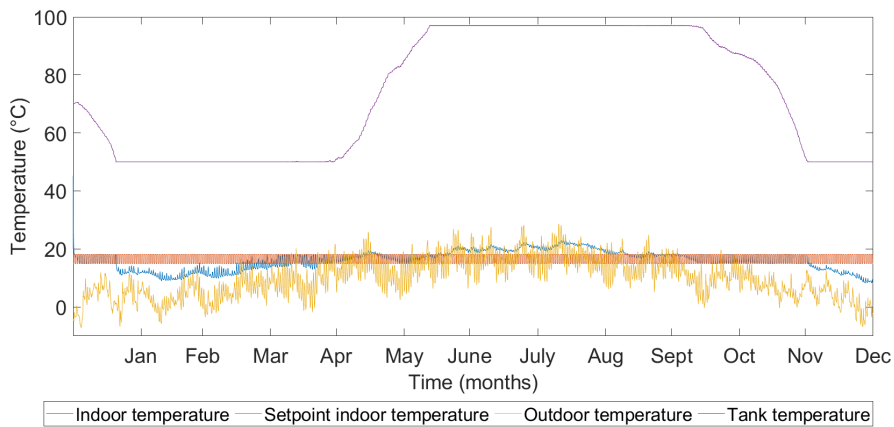


Figure 4.5: The yearly temperature variation for 1 PVT panel and 4 m^3 TESS capacity.

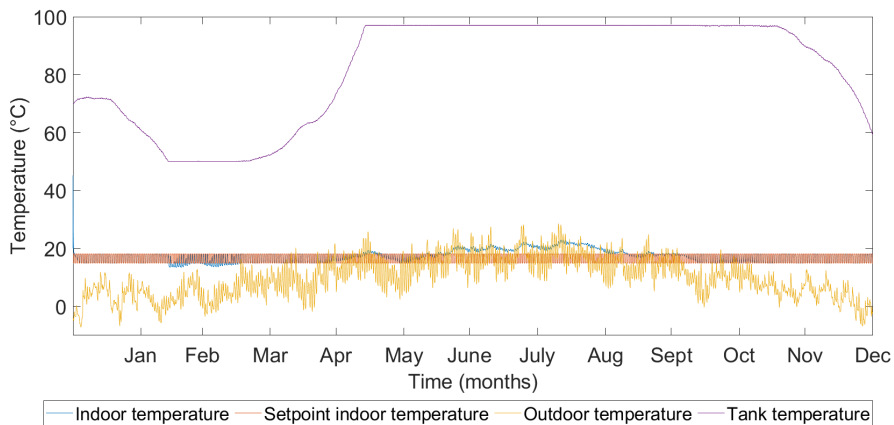


Figure 4.6: The yearly temperature variation for 3 PVT panels and 6 m^3 TESS capacity.

By comparing Figures 4.5 and 4.6, it can be observed that it takes longer for a larger system size for the TESS to charge and discharge. Also, for a larger system size, the period in which the tank is fully discharged is shorter, and the period in which the tank is fully charged is longer.

By analyzing Figures 4.7 and 4.8, it is apparent that for the larger system size, the indoor temperature is suitable throughout the entire year, whereas this is not true for the smaller system size. Furthermore, the observation is that in Figure 4.7, when the tank is fully discharged in springtime, the PVT panels generate enough heat to raise the indoor temperature to a tolerable level. On the other hand, this is not the case in wintertime when the indoor temperature is below comfortable standards.

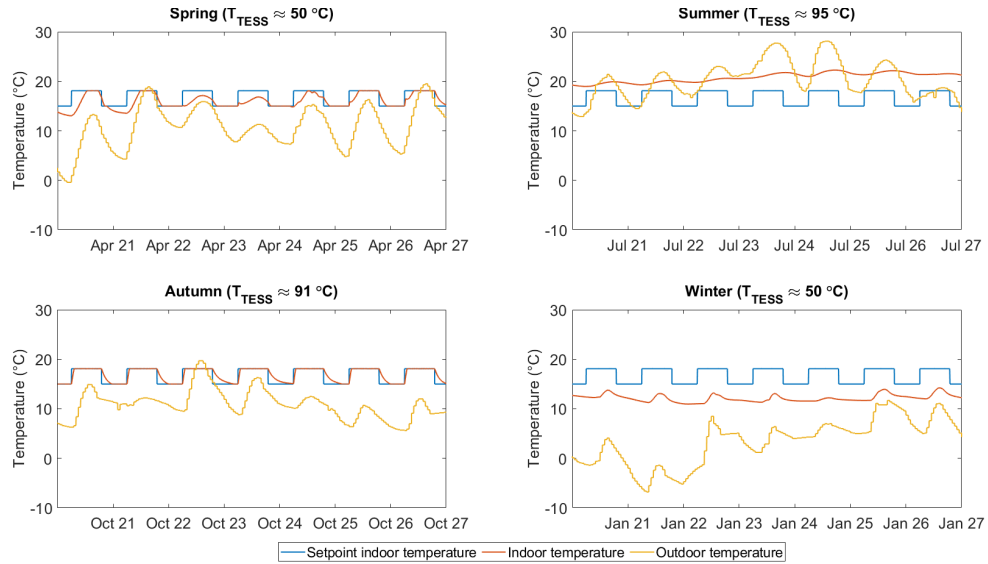


Figure 4.7: The seasonal temperature variation for 1 PVT panel and 4 m³ TESS capacity.

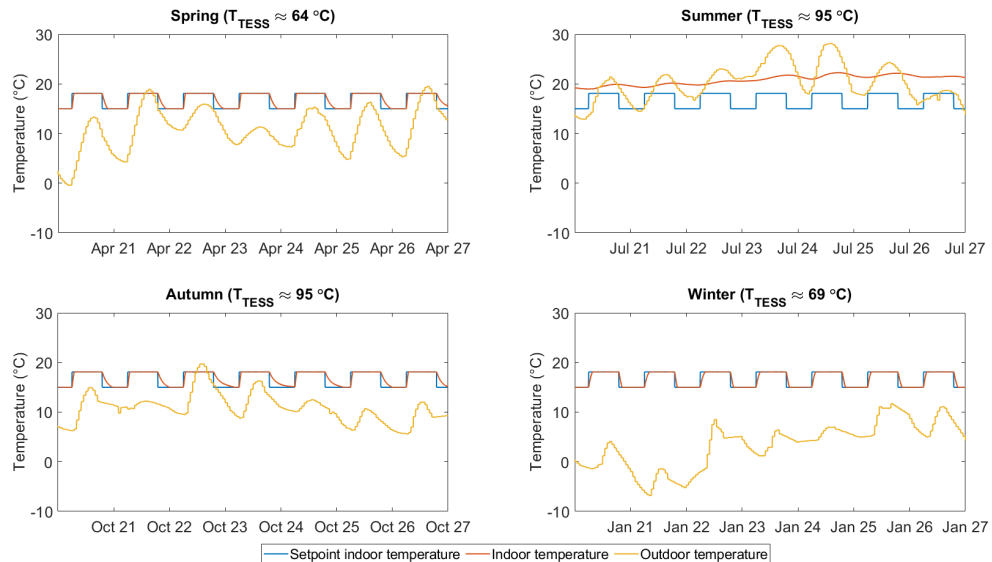


Figure 4.8: The seasonal temperature variation for 3 PVT panels and 6 m³ TESS capacity.

4.2.1 Payback Time

The number of uncomfortable days in the reference scenario with 0 PVT panels and no TESS capacity is 283. The resulting payback time, calculated using Equation 3.1 for each system size, can be seen in Figure 4.9. To calculate the avoided natural

gas consumption, the average yearly heat consumption in residential buildings of 9444 kWh [1] was used, because it gives a more realistic estimation of the payback time. It can be seen that the payback time is relatively constant for all system sizes with a TESS. Furthermore, there is a significant increase in payback time between the system sizes with and without a TESS. This increase results from the significant difference in initial costs between the PVT panels and the TESS.

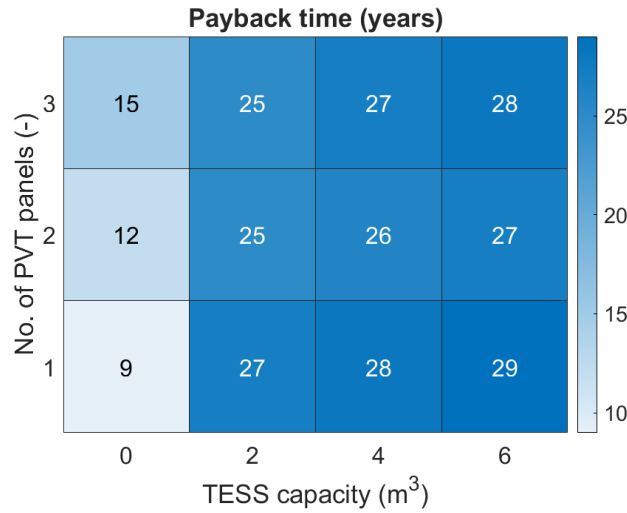


Figure 4.9: The years of payback time for each heating system size.

Figure 4.10 shows the CO₂ emissions for each PVT and TESS sizing, also determined using average yearly heat consumption in residential buildings of 9444 kWh. It demonstrates similar behaviour to Figure 4.4, which is expected because the more uncomfortable days, the more a boiler would be needed to assist the PVT and TESS, causing more emissions.

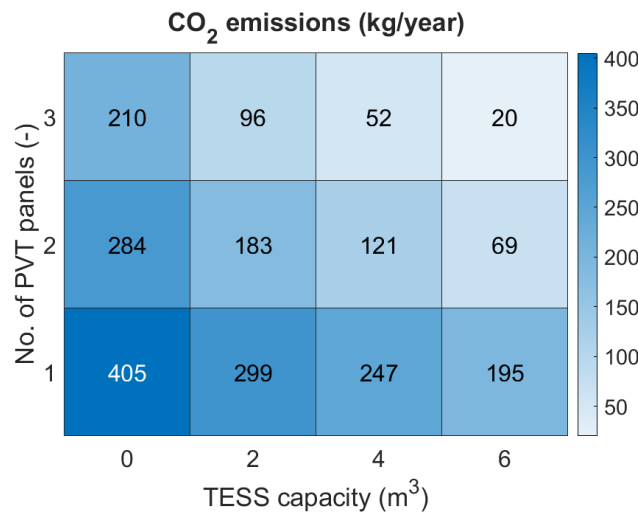


Figure 4.10: The CO₂ emissions for each heating system size.

4.3 SCENARIO III: PVT + TESS + HP

This Section presents results for scenario III, in which PVT panels heat the house, and a TESS buffers the intermittency of the PVT system. An HP was added as a tertiary heat source for periods when the PVT and TESS could not provide enough thermal energy.

Figures 4.11 and 4.12 show the temperature variation for the system sizing of 3 PVT panels and a buffer capacity of 6 m³. Furthermore, scenario III was modelled with 1 PVT panel and 4 m³ buffer capacity, and 3 PVT panels and 2 m³ buffer capacity. These sizes were chosen because they represent the extremes of system sizes. The results of the remaining system sizes can be seen in Appendix D.

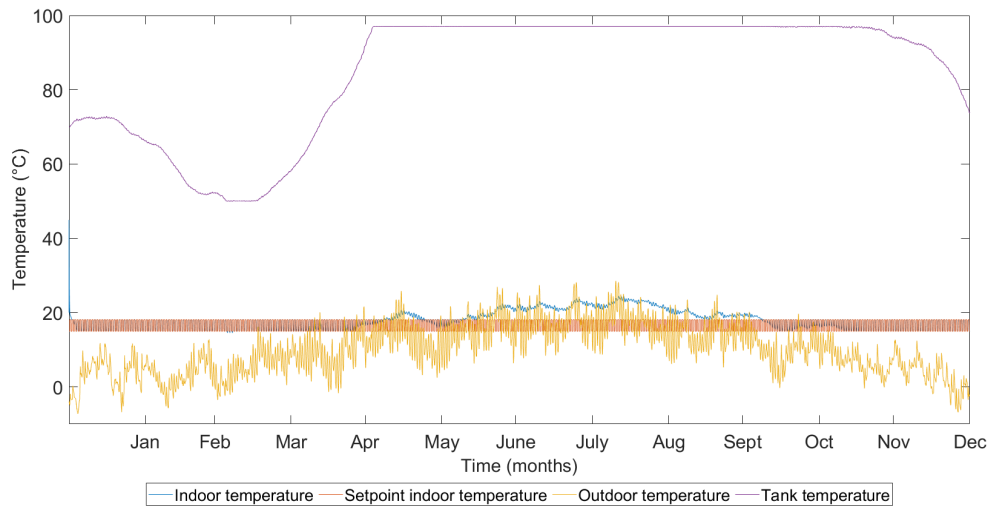


Figure 4.11: The yearly temperature variation for 3 PVT panels, 6 m³ TESS capacity, and a heat pump.

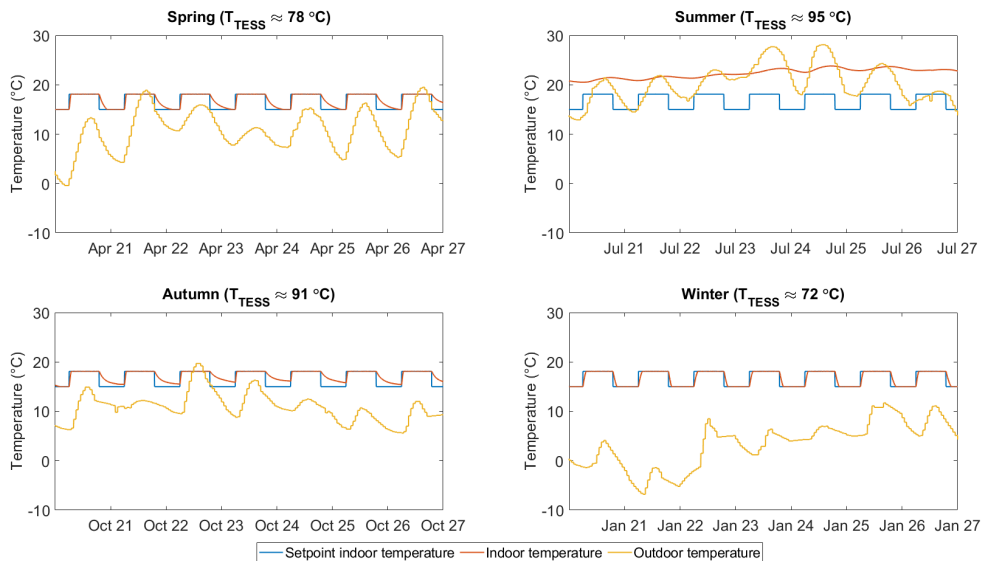


Figure 4.12: The seasonal temperature variation for 3 PVT panels, 6 m³ TESS capacity, and a heat pump.

From the yearly temperature in the tank in Figure 4.11 can be concluded that the tank is used for seasonal energy storage because the tank is fully discharged after colder months and fully charged after warmer months with higher solar irradiance.

Figure 4.13 shows the total heat flow every day of the year, in and out of the TESS. The tank is charged and discharged throughout the entire year, except when the tank is fully charged in summer. It can also be observed that the discharge rate is higher than the charge rate during winter and vice-versa during spring. Figures 4.11 and 4.13 show that the buffer tank is used for both seasonal and daily energy storage.

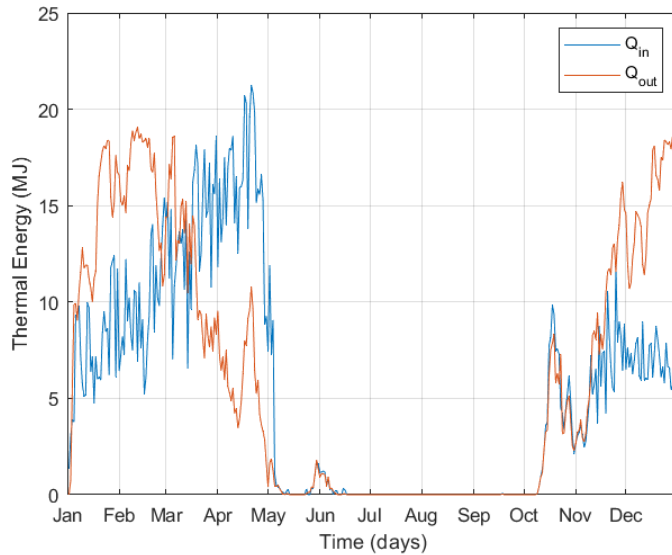


Figure 4.13: The total thermal energy exchanged by the TESS on each day of the year for 3 PVT panels, 6 m³ TESS capacity, and a heat pump.

Figure 4.14 quantifies the wasted thermal energy generated by the PVT panels. A waste ratio of 0 means that all generated thermal energy is either consumed directly or stored. A waste ratio of 1 means that none of the thermal energy generated on that day is consumed or stored. Figures 4.13 and 4.14 are based on data of the system with 3 PVT panels and 6 m³ TESS capacity.

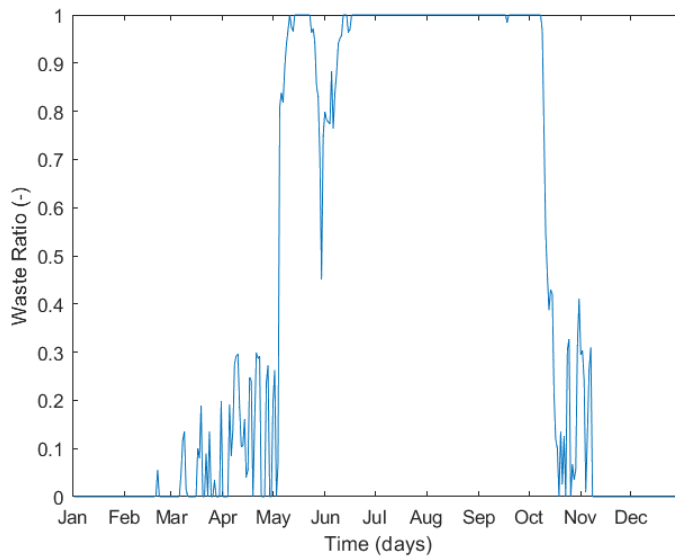


Figure 4.14: The ratio of thermal energy generated by the PVT panels that is wasted on each day of the year for 3 PVT panels, 6 m³ TESS capacity, and a heat pump.

5 | DISCUSSION

This Chapter discusses the method and results, generating insights into the limitations underlying the conducted research and putting them in perspective. Due to time restraints, modelling errors, and other reasons, some simplifications were made that limited the accuracy of the results. Section 5.1 covers these limitations and their influence on the results. Subsequently, the different scenarios are compared in Section 5.2, and the optimal buffer capacity is discussed in Section 5.3. Finally, installation requirements for thermal energy buffers are discussed in Section 5.4

5.1 MODEL LIMITATIONS

This Section discusses simplifications made by the created models and their possible effects. First of all, the model of the residential building will be addressed. Afterwards, the instability of the natural gas price is discussed, and finally, the model of the TESS is discussed.

5.1.1 Residential Heating System

In the model of the residential heating system, as discussed in Section 3.3.1, the following factors are not taken into account:

- Ventilation
- Heat transfer between neighboring houses
- Wind
- Radiative heat transfer to and from the ambient
- Domestic Hot Water (DHW) demand

As observed in the list above, the model does not account for all the house's thermal gains and losses. For example, the house's model does not consider ventilation, such as open windows, doors, and gaps or cracks. Moreover, heat transfer to neighbouring houses is not considered. Both factors are unpredictable, and obtaining representative data for them is challenging. Additionally, effects due to wind are neglected. The more wind and thus airflow around the house, the more convective heat transfer from the house to the ambient. Neglecting ventilation, heat transfer between neighbouring houses, and wind effects decrease the heat demand of the house.

In contrast, the model does not take into account radiation on windows, increasing the heat demand of the house. When solar irradiation on windows is high, radiation could account for a significant increase in indoor temperature. Neglecting the thermal losses due to ventilation and neighbouring houses could compensate for neglecting the thermal gains by radiation because people tend to open their windows on sunny days. However, this cannot be guaranteed. Furthermore, solar irradiance is more intermittent than thermal losses through cracks, gaps, and doors.

For simplicity, DHW demand is not considered. Data for DHW could be added to model peaks of hot water demand, to make the model more realistic. However, in a natural system, a closed tank that exchanges heat through heat exchangers has a reaction time that is too long to heat DHW. Therefore, if DHW demand is to be added

to the model, it cannot be satisfied by the TESS. A hot water tank should be added to satisfy the DHW demand. Optimally, this tank schedules filling according to the DHW demand.

5.1.2 Instability of the Natural Gas Price

The assumption on the natural gas price was based on the natural gas price in the second half of 2021. However, current geopolitical circumstances between Russia and Ukraine have caused the gas price to quadruple, as seen in Figure 5.1. The uncertainty of future gas prices causes a challenge in comparing the cost of electrified heating systems to traditional heating systems. It also confirms the need to decarbonize residential heating systems to secure comfortable, affordable housing.

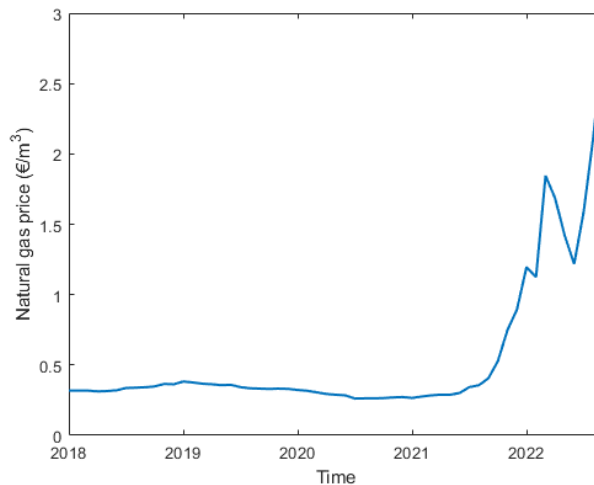


Figure 5.1: Average natural gas price for Dutch consumers. Data taken from [27].

5.1.3 TESS

The following assumptions are applied to the TESS model:

- Heat losses from the tank to the environment are neglected
- The temperature distribution inside the tank is uniform
- Permitted temperatures in the tank are a conservative estimate

According to Borg, the current estimated leakage rate is 100 W. The model neglects heat losses of the TESS, since research is currently done on the actual leakage rate. Furthermore, the heat losses from the tank to the ambient do not have a constant rate; they depend on the overall heat transfer coefficient, tank size, and temperature difference between the tank fluid and ambient, as illustrated by Equation 2.21. The overall heat transfer coefficient from the liquid in the tank to the ambient is unknown. Taking into account the heat losses would decrease the performance of the tank. The same quantity of stored thermal energy generated by the PVT would yield less useful thermal energy after storage. During summer, this would not have an effect on the heating system because enough thermal energy is generated by the PVT, as concluded from Figures 4.13 and 4.14.

The Simulink tank block assumes uniform temperature distribution throughout the tank. As stated in Section 2.3.2, a uniform temperature distribution does not represent the actual situation. Nevertheless, thermal stratification is minimal in the scope of this research since the stratification is only affected by heat exchange and not by fluid exchange.

The storage capacity of the TESS is estimated conservatively. The estimated permitted temperature range is relatively small compared to the range estimated by

Borg. A more extensive approved temperature range would increase the capacity of the tank, as can be concluded from Equation 2.12.

5.2 COMPARING SCENARIOS I, II AND III

This Section addresses the different scenarios and how they compare to one another. The indoor, outdoor, tank and ambient temperature variations for each scenario are presented in Sections 4.1 - 4.3.

The yearly heat consumption of the modelled house is 5109 kWh. This consumption is relatively low compared to 9444 kWh, which is the actual average heat consumption of a Dutch household. This difference could be caused by neglecting part of the house's heat losses, as explained in Section 5.1. The low heat demand is also influenced by the relatively low setpoint temperature of 18 °C during the day.

Scenarios I and III maintained a comfortable temperature during the entire year. The heating system of scenario II was insufficient to heat the house throughout the year for all modelled system sizes. It can be argued that the system could be suitable when larger PVT and TESS sizing are applied. However, a bigger tank would not be practical, and extra PVT panels would cause a sizeable yearly overproduction of thermal energy. A heat pump or infrared panels could be used when the heating system is insufficiently effective; the latter is preferable due to its low initial cost.

In terms of CO₂ emissions, most CO₂ is emitted in scenario I, namely 378 kg for a heating demand of 5109 kWh. In scenario II, CO₂ emissions are highly dependent on the sizing of the PVT system and the TESS and range from 20 to 405 kg, based on a heating demand of 9444 kWh. For scenario III, emissions depend on the ratio of different sources for electricity generation. Suppose the heat pump only uses electricity generated by solar panels or wind turbines. In that case, the emissions are eliminated, whereas electricity generated by fossil-fuelled power plants will contribute significantly to CO₂ emissions.

5.3 OPTIMAL BUFFER CAPACITY

This Section addresses the optimal capacity of the TESS based on costs and CO₂ emissions. When looking at Figures 4.10 and 4.9, it can be concluded that the optimal TESS capacity correlates with the amount of PVT panels. This correlation makes sense because there is more thermal energy to store with more PVT panels. Therefore, having a larger TESS capacity is more beneficial in combination with additional PVT panels.

When comparing Figures 4.10 and 4.9, it is evident that the CO₂ emissions are affected more by changing the buffer capacity than the payback time. The payback time is almost constant for each buffer size, while the CO₂ emissions drop significantly when the buffer capacity is increased. Considering the dependence on system size, CO₂ emissions were more crucial in determining the optimal buffer capacity than payback time. Therefore the optimal TESS capacity out of the investigated capacities is 6 m³. For a lower amount of CO₂ emissions and payback time, it is advised to pair the TESS with 3 PVT panels.

Intuitively, when looking at Figures 4.13 and 4.14, it seems inefficient that all thermal energy produced by the PVT panels is lost for almost half of the year. Nevertheless, the payback time of this system with 3 PVT panels and 6 m³ TESS capacity is still lower than the payback time of the system with only 1 PVT panel and 6 m³ TESS capacity, where less generated thermal energy will be lost.

5.4 TESS INSTALLATION REQUIREMENTS

To make a residential heating system compatible with a TESS, multiple factors must be considered. For example, to install such a device, the user needs to be a house owner owning a garden big enough to incorporate the tank. Furthermore, the appropriate infrastructure must be set up, such as pipes between the tank, PVT module, and heat pump. In addition, valves are needed to control the heating system to enable the tank's charging, discharging, and disconnecting.

To further demonstrate the installation requirements of a thermal energy buffer, Figure 5.2 and 5.3 show diagrams for power and thermal energy distribution in the household, respectively. It can be observed that to install a heat pump, additional components such as pipes and a power security breaker are needed, in addition to an indoor and outdoor unit. The indoor and outdoor units must be placed close to each other to prevent heat loss.

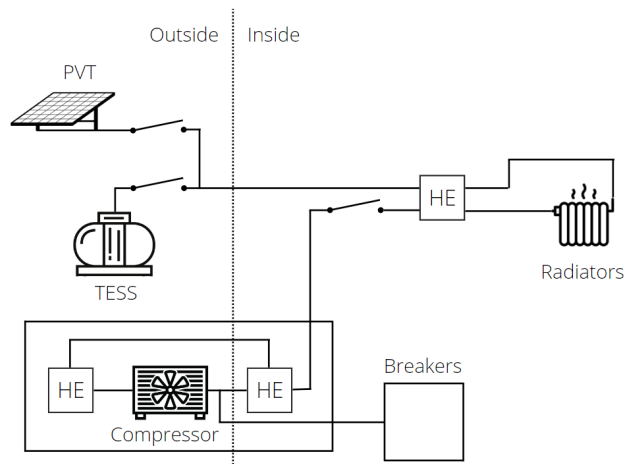


Figure 5.2: Heat distribution diagram in the modelled residential building.

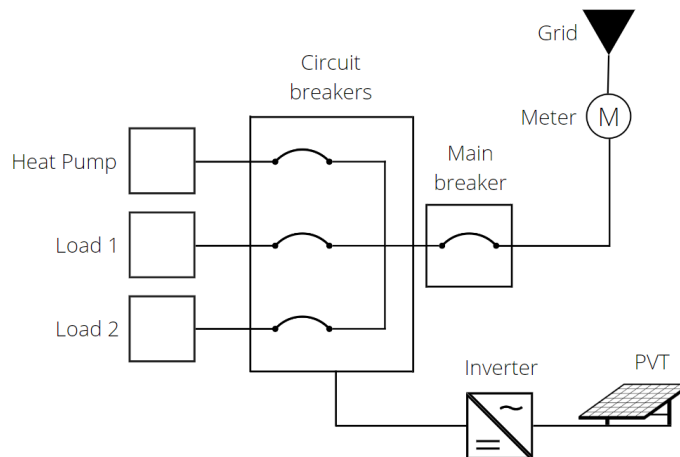


Figure 5.3: Power distribution diagram in the modelled residential building.

6 | CONCLUSIONS

Concluding this thesis report, this Chapter will respond to the research questions by summarising earlier content of the report. Furthermore, recommendations will be made for further research.

Research Questions

- What are the requirements to make a heating system compatible with a thermal energy buffer?

To install a thermal energy buffer, the user must be a homeowner with a garden large enough to accommodate the tank. The necessary infrastructure must be installed, including pipes connecting the heat pump, PVT module, and tank. Additionally, valves are required to regulate the heating system so the tank can be charged, discharged, and disconnected.

- What is the optimal way of using a thermal energy buffer in terms of storage and consumption conditions to minimise costs?

For a household with an average heating demand of 9444 kWh, the lowest payback time was found for a TESS capacity of 2 m³, in combination with 2 or 3 PVT panels. Moreover, the payback time of a thermal energy buffer is shorter in homes with higher space heating energy consumption because there are more variable costs that can be avoided.

- What are the differences in energy use of households that generate thermal energy for space heating (I) using a traditional heating system with a boiler, (II) with PVT modules and a thermal buffer, and (III) with PVT modules, thermal buffer and heat pump?

The residential heating systems of scenarios I and III were able to secure a comfortable indoor temperature throughout the year. In contrast, this was not the case for the heating system of scenario II.

Scenario I produces the most CO₂ emissions, 378 kg for a heating demand of 5109 kWh. Based on a heating demand of 9444 kWh, scenario II's CO₂ emissions range from 20 to 405 kg and are highly dependent on the PVT system and TESS sizes. For scenario III, CO₂ emissions depend on the ratio of different sources for electricity generation.

- Considering volumetric constraints, what is the optimal capacity of a thermal energy buffer that minimises costs and CO₂ emissions?

Changing the buffer capacity has a more significant impact on CO₂ emissions than on the payback time. Therefore, CO₂ emissions were more critical than payback time in determining the ideal buffer capacity. In light of this, 6 m³ is the optimal TESS capacity among the capacities examined. Combining the TESS with 3 PVT panels is suggested for a reduced amount of CO₂ emissions and payback time.

Recommendations

Given the mentioned results and their conclusions, several recommendations can be made that would be interesting starting points for future research.

For example, one could study the effect of a house's energy label on the optimal heating system configuration, look at the feasibility of larger TESS capacities or sharing a TESS among neighbouring households, or investigate the behaviour of the model if cooling technologies are added.

Besides, the effect of different setpoint temperature profiles could be explored. For example, a higher setpoint temperature during the day or another daily profile of elevated indoor temperature could be studied.

Moreover, one could look into the consequences of adding DHW demand to the model. It could be combined with exchanging the PVT system in scenarios II and III for solar thermal collectors and adding a hot water tank, allowing higher operating temperatures and steeper ramping rates needed for DHW. Furthermore, the difference between closed and open thermal energy buffer tanks could be compared.

It might also be interesting to examine the economic effects of charging a thermal buffer with heat from a heat pump when the electricity price is low. Also, the impact of such conditional charging behaviour on the electricity network could be reviewed. Moreover, one could investigate how to coordinate electrical power safety in a household where a heat pump is to be installed.

Finally, the effect of the heat exchanger coils' geometry on the storage performance and distribution of thermal energy inside the tank could be considered. Additionally, the ratio between the depth and width of the tank and its effect on the storage performance could be studied.

BIBLIOGRAPHY

- [1] IEA. *Key Energy Statistics*. 2022. URL: <https://www.iea.org/countries/the-netherlands>.
- [2] Kunal Chowdhury. *Decarbonising the Residential Space Heating Sector of the Netherlands in 2050 through Three Decarbonisation Pathways-Hydrogen Boilers, Hybrid Heat Pumps and Electric Heat Pumps*. Tech. rep. 2020. URL: <http://repository.tudelft.nl/>.
- [3] Luigi Schibuola, Massimiliano Scarpa, and Chiara Tambani. "Demand response management by means of heat pumps controlled via real time pricing". In: *Energy and Buildings* 90 (Mar. 2015), pp. 15–28. ISSN: 03787788. DOI: [10.1016/j.enbuild.2014.12.047](https://doi.org/10.1016/j.enbuild.2014.12.047).
- [4] Martin Rüdüsüli, Sinan L. Teske, and Urs Elber. "Impacts of an increased substitution of fossil energy carriers with electricity-based technologies on the Swiss electricity system". In: *Energies* 12.12 (2019). ISSN: 19961073. DOI: [10.3390/en12122399](https://doi.org/10.3390/en12122399).
- [5] Mitch Geraedts et al. "Optimal Sizing of a Community Level Thermal Energy Storage System". In: *2022 IEEE 21st Mediterranean Electrotechnical Conference (MELECON)*. 2022, pp. 52–57. DOI: [10.1109/MELECON53508.2022.9842945](https://doi.org/10.1109/MELECON53508.2022.9842945).
- [6] Borg. *Verwarm je huis. Niet de Planeet*. 2022. URL: borg.energy.
- [7] Theodore L Bergman et al. *Introduction to heat transfer*. John Wiley & Sons, 2011. ISBN: 0470501960.
- [8] Mudde R and van den Akker H. *Fysische Transportverschijnselen*. 4th ed. Delft: VSSD, 2014.
- [9] Smets A et al. *Solar energy: The physics and engineering of photovoltaic conversion, technologies and systems*. Cambridge, England: UIT, 2015.
- [10] J W J Westendorp. "The central heating boiler in the past, present and the future. De cv-ketel van toen, nu en in de toekomst." In: 50:1 (Jan. 1993).
- [11] Swapan Basu and Ajay Kumar Debnath. "Coordinated Control System". In: *Power Plant Instrumentation and Control Handbook* (2015), pp. 749–766. DOI: [10.1016/B978-0-12-800940-6.00010-1](https://doi.org/10.1016/B978-0-12-800940-6.00010-1).
- [12] K. J. Chua, S. K. Chou, and W. M. Yang. "Advances in heat pump systems: A review". In: *Applied Energy* 87.12 (Dec. 2010), pp. 3611–3624. ISSN: 0306-2619. DOI: [10.1016/J.APENERGY.2010.06.014](https://doi.org/10.1016/J.APENERGY.2010.06.014).
- [13] HJ Laue and K Heinloth. *9 Heat pumps*. Tech. rep. 2006.
- [14] Olaia Eguiarte et al. "Energy, environmental and economic analysis of air-to-air heat pumps as an alternative to heating electrification in Europe". In: *Energies* 13.15 (Aug. 2020). ISSN: 19961073. DOI: [10.3390/en13153939](https://doi.org/10.3390/en13153939).
- [15] Iain Staffell et al. "A review of domestic heat pumps". In: *Energy & Environmental Science* 5.11 (2012), pp. 9291–9306.
- [16] Hans Ludwig Von Cube and Fritz Steimle. *Heat pump technology*. Elsevier, 2013. ISBN: 1483102475. URL: https://books.google.nl/books?hl=nl&lr=&id=YNH8BAAAQBAJ&oi=fnd&pg=PP1&dq=heat+pump&ots=Ev9uKT7ope&sig=GhVezVXvlkbq1MAXoLkDepNgpBs&redir_esc=y#v=onepage&q=heat%20pump&f=false.
- [17] Rokas Valancius et al. *A review of heat pump systems and applications in cold climates: Evidence from Lithuania*. Nov. 2019. DOI: [10.3390/en12224331](https://doi.org/10.3390/en12224331).

- [18] The Engineering ToolBox. *Refrigerants - Physical Properties*. 2005. URL: https://www.engineeringtoolbox.com/refrigerants-d_902.html.
- [19] T T Chow, J Ji, and W He. "Photovoltaic-thermal collector system for domestic application". In: (2007). ISSN: 0199-6231.
- [20] Ahmad Fudholi et al. "Performance analysis of photovoltaic thermal (PVT) water collectors". In: *Energy Conversion and Management* 78 (Feb. 2014), pp. 641–651. ISSN: 0196-8904. DOI: [10.1016/J.ENCONMAN.2013.11.017](https://doi.org/10.1016/J.ENCONMAN.2013.11.017).
- [21] the free encyclopedia Wikipedia. *Photovoltaic thermal hybrid solar collector*. URL: https://en.wikipedia.org/wiki/Photovoltaic_thermal_hybrid_solar_collector.
- [22] Sandeep S. Joshi and Ashwinkumar S. Dhoble. "Photovoltaic -Thermal systems (PVT): Technology review and future trends". In: *Renewable and Sustainable Energy Reviews* 92 (Sept. 2018), pp. 848–882. ISSN: 1364-0321. DOI: [10.1016/J.RSER.2018.04.067](https://doi.org/10.1016/J.RSER.2018.04.067).
- [23] Mohamed Hissouf et al. "Effect of optical, geometrical and operating parameters on the performances of glazed and unglazed PV/T system". In: *Applied Thermal Engineering* 197 (Oct. 2021), p. 117358. ISSN: 1359-4311. DOI: [10.1016/J.APPLTHERMALENG.2021.117358](https://doi.org/10.1016/J.APPLTHERMALENG.2021.117358).
- [24] Li G et al. "Solar energy utilisation: Current status and roll-out potential". In: *Applied Thermal Engineering* 209 (June 2022), p. 118285. ISSN: 1359-4311. DOI: [10.1016/J.APPLTHERMALENG.2022.118285](https://doi.org/10.1016/J.APPLTHERMALENG.2022.118285).
- [25] ArabiaWeather. *Smart heating panels*. 2022. URL: <https://www.arabiaweather.com/en/content/smart-heating-panels>.
- [26] Alibaba.com. *Amazon Heaters Infrared Wall Picture*. URL: https://www.alibaba.com/product-detail/amazon-heaters-infrared-wall-picture-UV_877102016.html.
- [27] Centraal Bureau voor de Statistiek. *Huishoudens nu*. 2022. URL: <https://www.cbs.nl/nl-nl/visualisaties/dashboard-bevolking/woonsituatie/huishoudens-nu#:~:text=Hoeveel%20huishoudens%20zijn%20er%20in,gemiddelde%20huishoudensgrootte%20nog%203%2C54..>
- [28] Simona Marinelli et al. "Life Cycle Thinking (LCT) applied to residential heat pump systems: A critical review". In: *Energy and Buildings* 185 (Feb. 2019), pp. 210–223. ISSN: 0378-7788. DOI: [10.1016/J.ENBUILD.2018.12.035](https://doi.org/10.1016/J.ENBUILD.2018.12.035).
- [29] Andrea Mangel Raventos et al. "Modeling the Performance of an Integrated Battery and Electrolyzer System". In: *Industrial & Engineering Chemistry Research* 60.30 (Aug. 2021), pp. 10988–10996. ISSN: 0888-5885. DOI: [10.1021/acs.iecr.1c00990](https://doi.org/10.1021/acs.iecr.1c00990). URL: <https://doi.org/10.1021/acs.iecr.1c00990>.
- [30] Spyros Giannelos et al. "Quantification of the energy storage contribution to security of supply through the F-factor methodology". In: *Energies* 13.4 (2020). ISSN: 19961073. DOI: [10.3390/en13040826](https://doi.org/10.3390/en13040826).
- [31] Gabriele Fambri et al. "Demand flexibility enabled by virtual energy storage to improve renewable energy penetration". In: *Energies* 13.19 (Oct. 2020). ISSN: 19961073. DOI: [10.3390/en13195128](https://doi.org/10.3390/en13195128).
- [32] Henrik Brynthe Lund et al. "Energy Storage and Smart Energy Systems". In: *International Journal of Sustainable Energy Planning and Management* 11 (2016), pp. 3–14.
- [33] Yu Li, Yacine Rezgui, and Hanxing Zhu. *District heating and cooling optimization and enhancement – Towards integration of renewables, storage and smart grid*. 2017. DOI: [10.1016/j.rser.2017.01.061](https://doi.org/10.1016/j.rser.2017.01.061).
- [34] Jay Hennessy et al. "Flexibility in thermal grids: A review of short-term storage in district heating distribution networks". In: *Energy Procedia*. Vol. 158. Elsevier Ltd, 2019, pp. 2430–2434. DOI: [10.1016/j.egypro.2019.01.302](https://doi.org/10.1016/j.egypro.2019.01.302).

- [35] Ioan Sarbu and Calin Sebarchievici. *A comprehensive review of thermal energy storage*. Jan. 2018. DOI: [10.3390/su10010191](https://doi.org/10.3390/su10010191).
- [36] Harry Mahon et al. *A review of thermal energy storage technologies for seasonal loops*. Jan. 2022. DOI: [10.1016/j.energy.2021.122207](https://doi.org/10.1016/j.energy.2021.122207).
- [37] K. Edem N'Tsoukpoe et al. "A review on long-term sorption solar energy storage". In: *Renewable and Sustainable Energy Reviews* 13.9 (Dec. 2009), pp. 2385–2396. ISSN: 1364-0321. DOI: [10.1016/J.RSER.2009.05.008](https://doi.org/10.1016/J.RSER.2009.05.008).
- [38] Thomas Schmidt et al. "Design Aspects for Large-scale Pit and Aquifer Thermal Energy Storage for District Heating and Cooling". In: *Energy Procedia* 149 (Sept. 2018), pp. 585–594. ISSN: 1876-6102. DOI: [10.1016/J.EGYPRO.2018.08.223](https://doi.org/10.1016/J.EGYPRO.2018.08.223).
- [39] Gang Li. "Sensible heat thermal storage energy and exergy performance evaluations". In: *Renewable and Sustainable Energy Reviews* 53 (Jan. 2016), pp. 897–923. ISSN: 1364-0321. DOI: [10.1016/J.RSER.2015.09.006](https://doi.org/10.1016/J.RSER.2015.09.006).
- [40] Engineering Community. "Summary of Valve Types". In: (). URL: <https://engineerscommunity.com/t/summary-of-valve-types/7426>.
- [41] K Chopra et al. "Recent advancement in heat pipe for stationary solar collectors". In: *IET Conference Publications*. Vol. 2018. CP749. 2018. URL: <https://www.scopus.com/inward/record.uri?eid=2-s2.0-85061375373&partnerID=40&md5=c0664f20d02fdb4547d0fe5647fae976>.
- [42] David Reay, Ryan McGlen, and Peter Kew. *Heat pipes: theory, design and applications*. Butterworth-Heinemann, 2013. ISBN: 0080982794. URL: https://books.google.nl/books?hl=nl&lr=&id=_G2SIYmFLEAC&oi=fnd&pg=PP1&dq=heat+pipes&ots=L8N0bH1YjM&sig=BNFabYj5dHD6OyGNlpubaHbssDs&redir_esc=y#v=onepage&q&f=false.
- [43] cooliance. *Heatpipe Technology*. 2019. URL: <http://www.cooliance.com/NA/Technologies/Heat-Pipes/index.php>.
- [44] Faghri A. "Heat pipes: review, opportunities and challenges". In: *Frontiers in Heat Pipes (FHP)* 5.1 (2014). DOI: [10.5098/fhp.5.1](https://doi.org/10.5098/fhp.5.1).
- [45] S. M. Khairnasov and A. M. Naumova. "Heat pipes application to solar energy systems". In: *Applied Solar Energy (English translation of Geliotekhnika)* 52.1 (Jan. 2016), pp. 47–60. ISSN: 0003701X. DOI: [10.3103/S0003701X16010060](https://doi.org/10.3103/S0003701X16010060).
- [46] Bosch Thermotechnik GmbH. *Datasheet Compress ODU Split 4*. 2021.
- [47] Marlon Schlemminger et al. "Dataset on electrical single-family house and heat pump load profiles in Germany". In: *Scientific Data* 9.1 (Dec. 2022). ISSN: 20524463. DOI: [10.1038/s41597-022-01156-1](https://doi.org/10.1038/s41597-022-01156-1).
- [48] Koninklijk Nederlands Meteorologisch Instituut (KNMI). *Klimaatdashboard*. 2022. URL: <https://www.knmi.nl/klimaatdashboard>.
- [49] Rijksdienst voor Ondernemend Nederland. *Energielabel woningen*. Tech. rep. 2021.
- [50] Inc. The MathWorks. *House Heating System*. 2022. URL: <https://nl.mathworks.com/help/physmod/hydro/ug/house-heating-system.html>.
- [51] World Health Organization. *Indoor environment: Health aspects of air quality, thermal environment, light and noise*. Tech. rep. 1990, p. 17.
- [52] The MathWorks Inc. *Photovoltaic Thermal (PV/T) Hybrid Solar Panel*. 2022. URL: <https://nl.mathworks.com/help/physmod/sps/ug/photovoltaic-thermal-pvt-hybrid-solar-panel.html>.
- [53] Centraal Bureau voor de Statistiek (CBS). "Average energy prices for consumers". In: (). URL: <https://www.cbs.nl/en-gb/figures/detail/84672ENG>.

- [54] Wiebke Meesenburg, Torben Ommen, and Brian Elmegaard. “Dynamic exergoeconomic analysis of a heat pump system used for ancillary services in an integrated energy system”. In: *Energy* 152 (June 2018), pp. 154–165. ISSN: 03605442. DOI: [10.1016/j.energy.2018.03.093](https://doi.org/10.1016/j.energy.2018.03.093).

A

HOUSE PARAMETERS

This appendix contains all defined parameters, such as the dimensions and material properties of the house. These parameters are divided over tables Table A.1-A.3, with parameters for the wall, windows and roof, respectively.

Table A.1: House parameters considering the walls.

Variable	Value	Unit
House length	15	m
House width	8	m
House height	2.6	m
Thickness of wall	0.25	m
Density of concrete	2400	kg/m ³
Specific heat of concrete	750	J/kgK
Thermal conductivity of concrete	0.14	W/mK
Convective heat transfer coefficient from indoor to wall	0.9 ¹	W/m ² K
Convective heat transfer coefficient from wall to outdoor	0.9 ¹	W/m ² K

¹ This value is not realistic, as it was scaled to reach an overall heat transfer coefficient of 2.14 m²K/W. This is an average value for a residential building with energy label C [49].

Table A.2: House parameters considering the windows.

Variable	Value	Unit
Number of windows in room 1	3	-
Number of windows in room 2	2	-
Number of windows in room 3	2	-
Number of windows in room 4	1	-
Height of windows	1	m
Width of windows	1	m
Thickness of single window pane	0.004	m
Thickness of cavity between panes	0.014	m
Density of glass	2500	kg/m ³
Specific heat of glass	840	J/kgK
Thermal conductivity of glass	0.8	W/mK
Convective heat transfer coefficient from indoor to glass	25	W/m ² K
Convective heat transfer coefficient from glass to outdoor	32	W/m ² K

Table A.3: House parameters considering the roof.

Variable	Value	Unit
Pitch of roof	40	°
Thickness of roof	0.2	m
Density of glass fiber	2440	kg/m ³
Specific heat of glass fiber	835	J/kgK
Thermal conductivity of glass fiber	0.04	W/mK
Convective heat transfer coefficient from indoor to roof	12	W/m ² K
Convective heat transfer coefficient from roof to outdoor	38	W/m ² K

B | ADDITIONAL RESULTS SCENARIO I

This appendix contains additional results of scenario I, the scenario in which the house is heated by a gas boiler. The output of the boiler is based on mass flow data for 10000 households, scaled down to a single household. This data was provided by Sweco. It was decided not to use these results in the main report since averaged data is less representative than data for a single case. Data for a single case would have more extreme data points compared to averaged data.

The Simulink model that was used is shown in Figure B.1, the input data in Figure B.2 and the results in Figure B.3 and B.4.

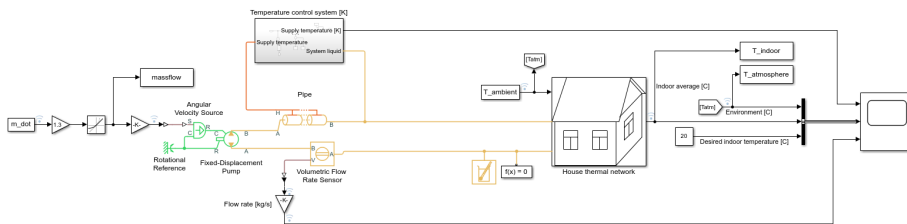


Figure B.1: Simulink model for scenario I based on mass flow input data.

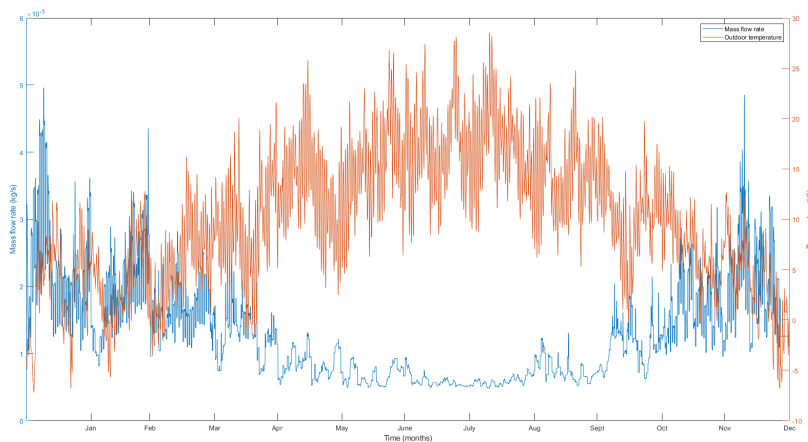


Figure B.2: Data input.

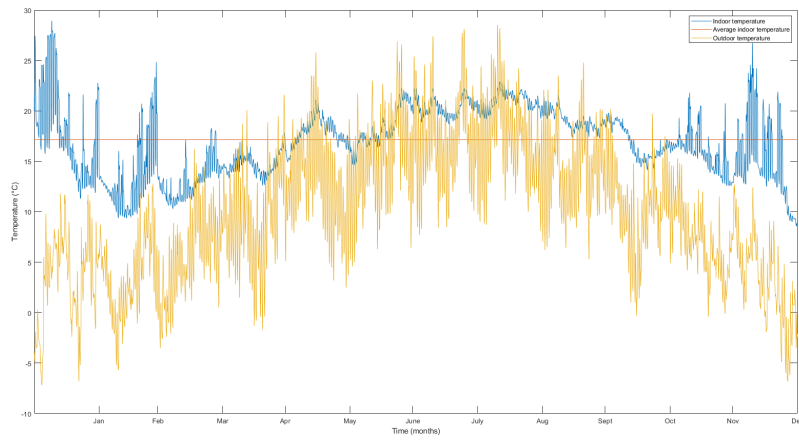


Figure B.3: Yearly outdoor and resulting indoor temperature variation.

The yearly average indoor temperature is 17.1 °C. A more zoomed-in version can be seen in Figure B.4.

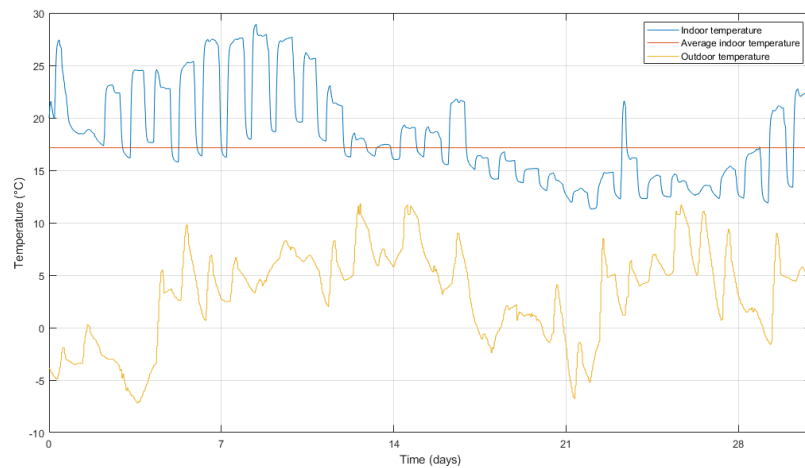


Figure B.4: Monthly temperature variation in January.

An expected profile would be a temperature around 20 °C during daytime and 15 °C during nighttime. From the results in Figure B.4 can be concluded that this was not always the case. These variations are possibly caused by weekends or holidays when more people generally spent time at home and therefore consume more heat.

C

ADDITIONAL RESULTS SCENARIO II

This appendix contains additional results of scenario II. In this scenario, the house is heated by a PVT module and a thermal energy buffer.

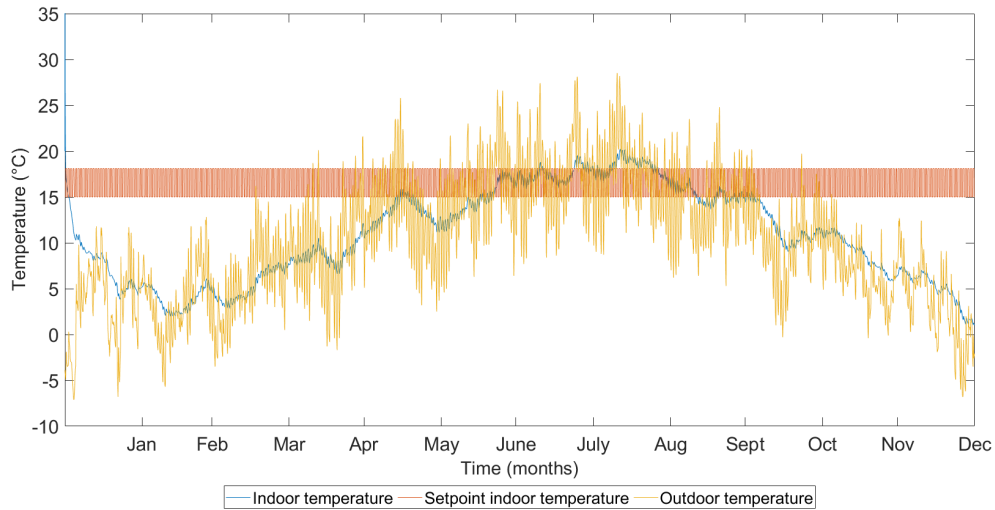


Figure C.1: The yearly temperature variation for 0 PVT panels and 0 m³ TESS capacity.

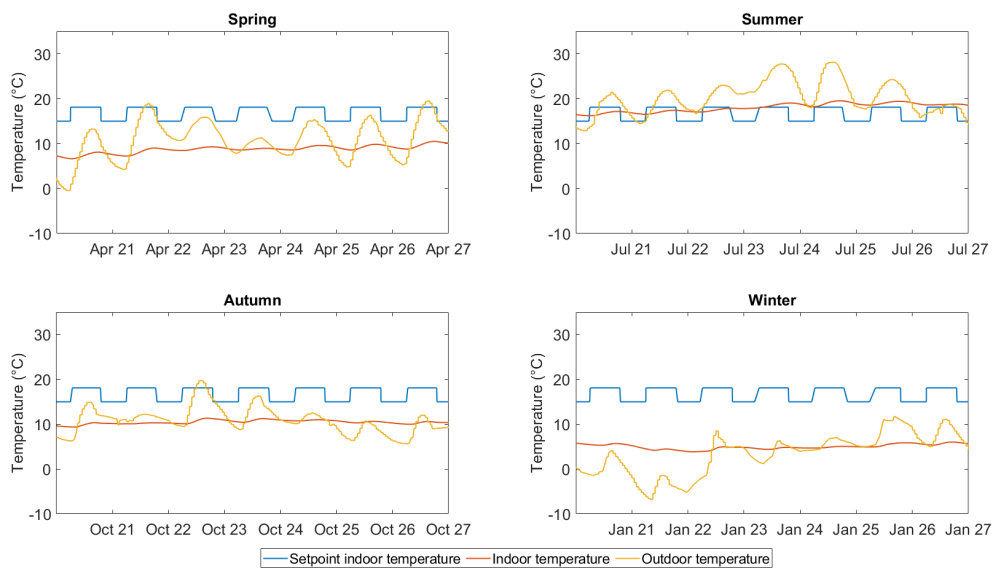


Figure C.2: The seasonal temperature variation for 0 PVT panels and 0 m³ TESS capacity.

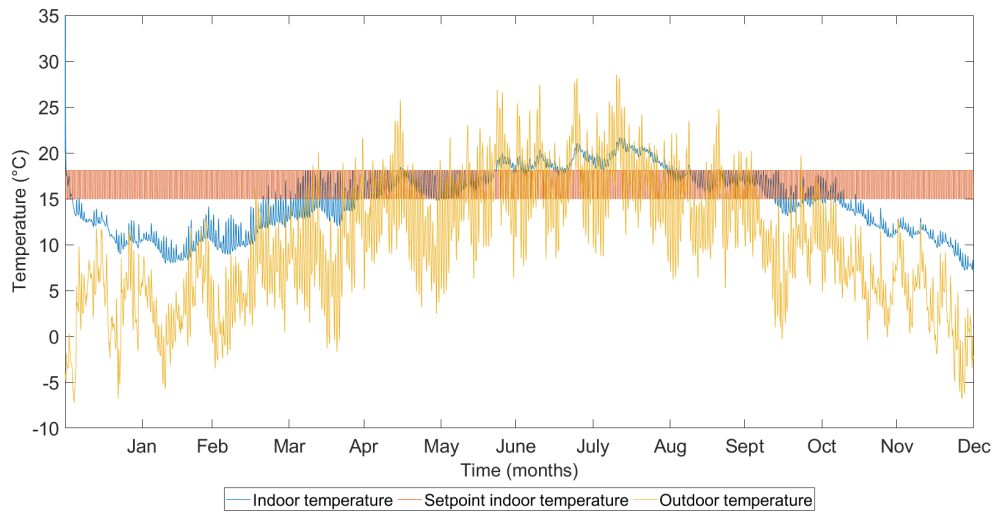


Figure C.3: The yearly temperature variation for 1 PVT panel and 0 m³ TESS capacity.

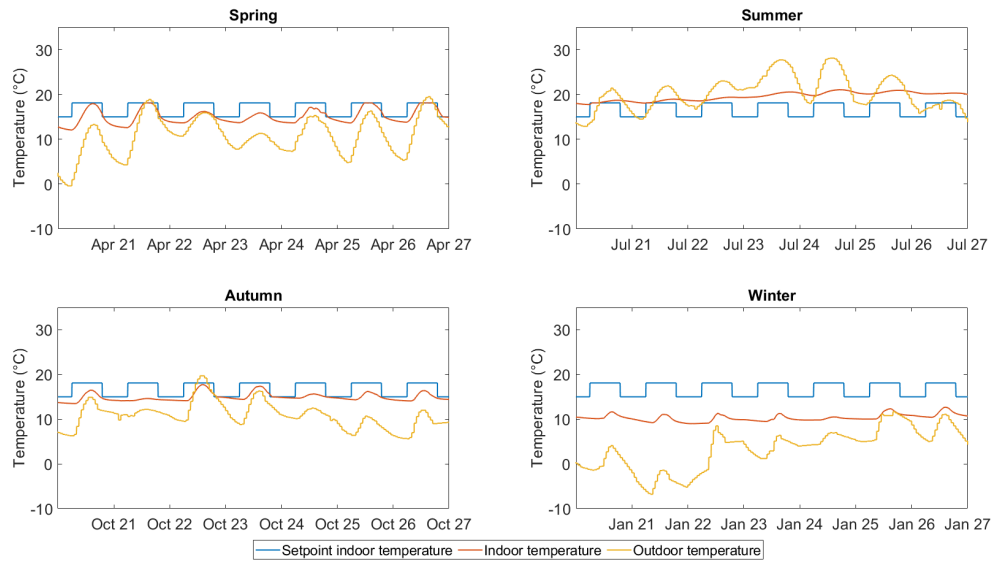


Figure C.4: The seasonal temperature variation for 1 PVT panel and 0 m³ TESS capacity.

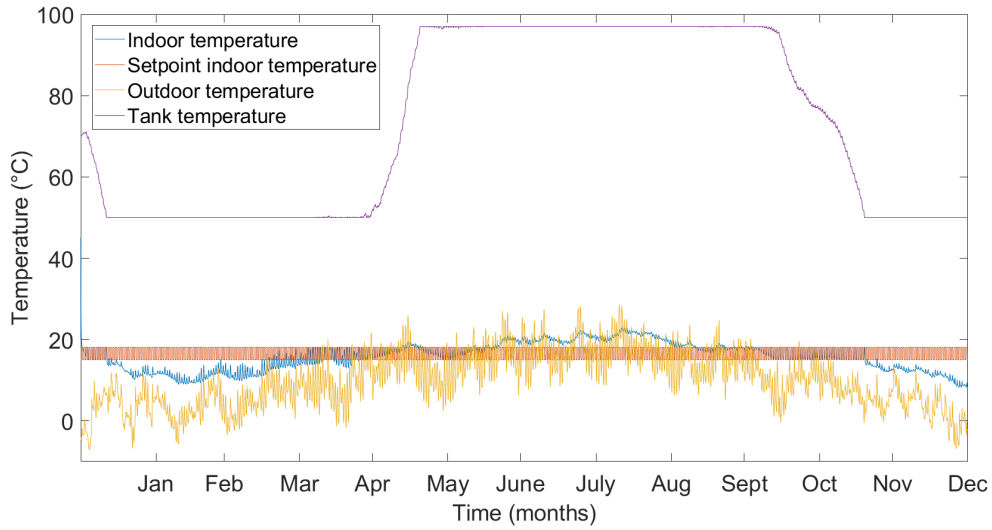


Figure C.5: The yearly temperature variation for 1 PVT panel and 2 m³ TESS capacity.

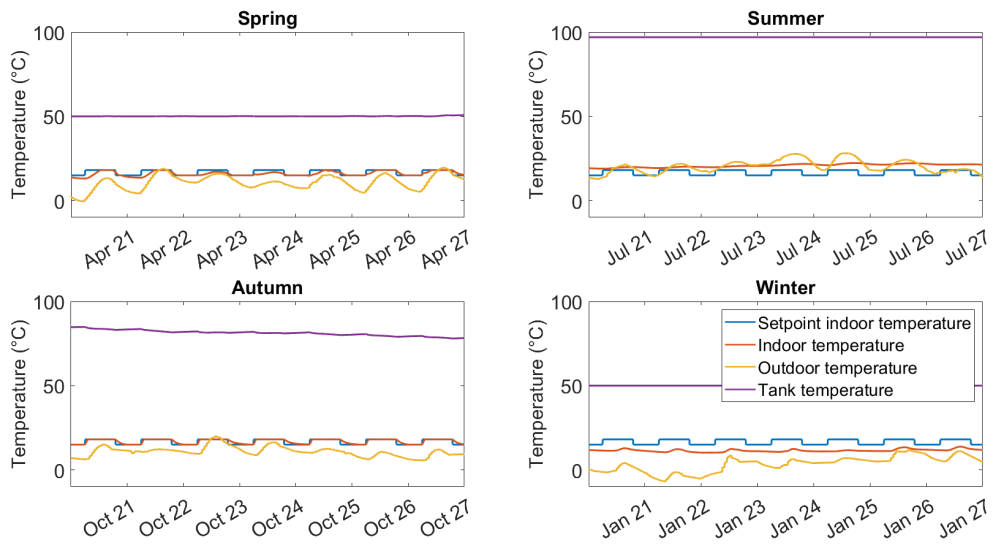


Figure C.6: The seasonal temperature variation for 1 PVT panel and 2 m³ TESS capacity.

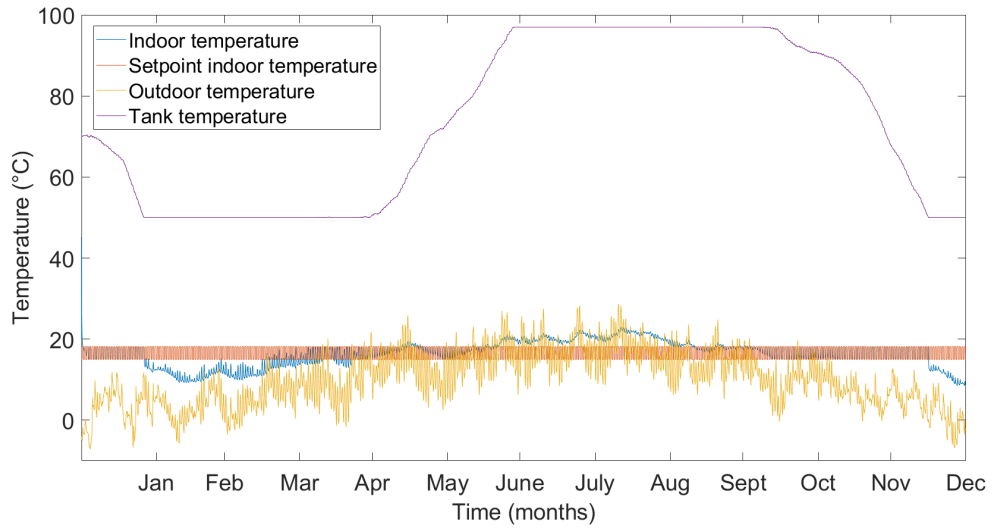


Figure C.7: The yearly temperature variation for 1 PVT panel and 6 m³ TESS capacity.

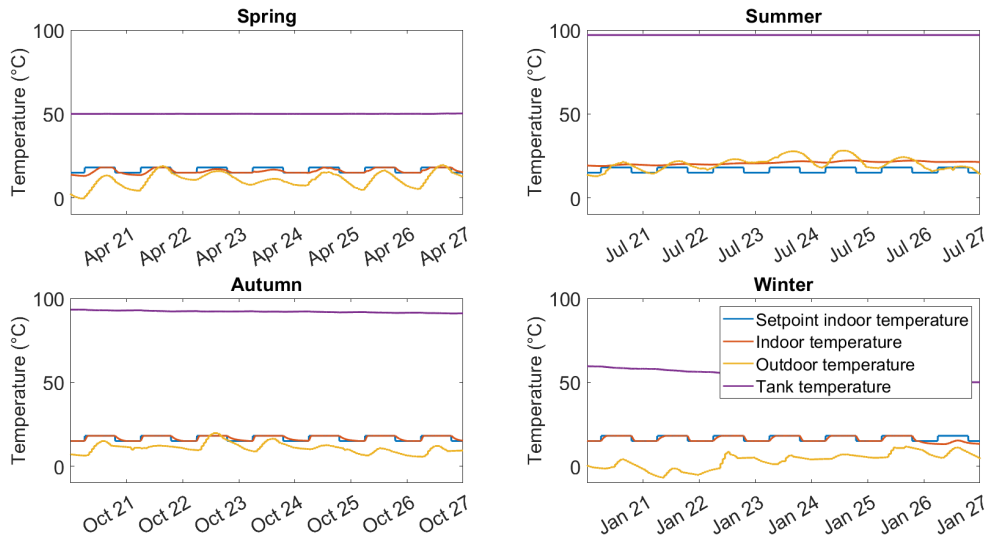


Figure C.8: The seasonal temperature variation for 1 PVT panel and 6 m³ TESS capacity.

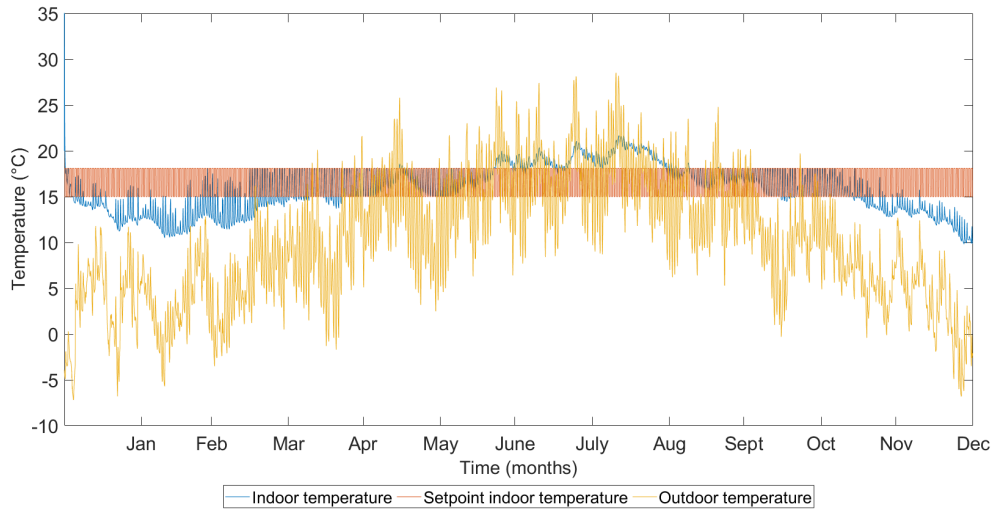


Figure C.9: The yearly temperature variation for 2 PVT panels and 0 m³ TESS capacity.

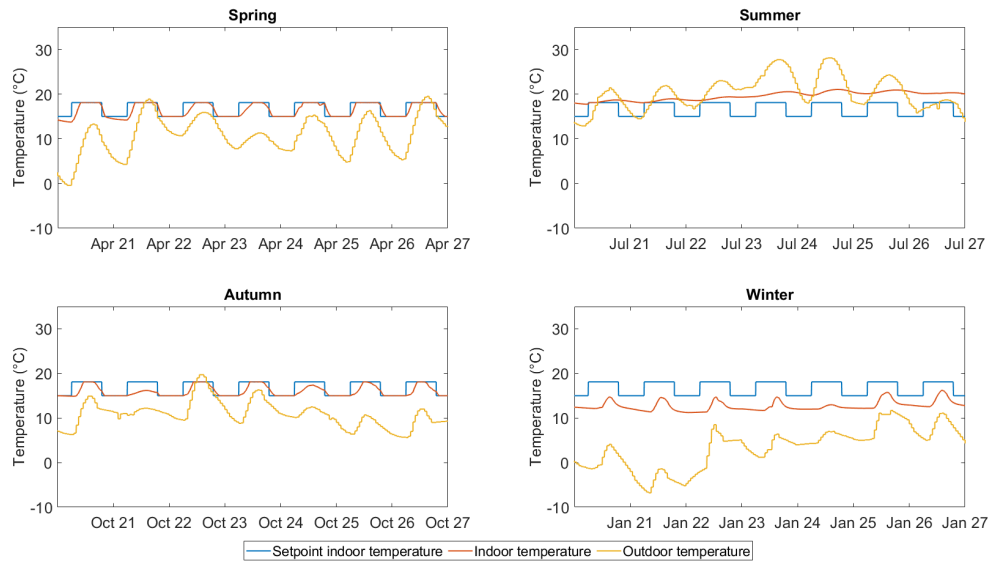


Figure C.10: The seasonal temperature variation for 2 PVT panels and 0 m³ TESS capacity.

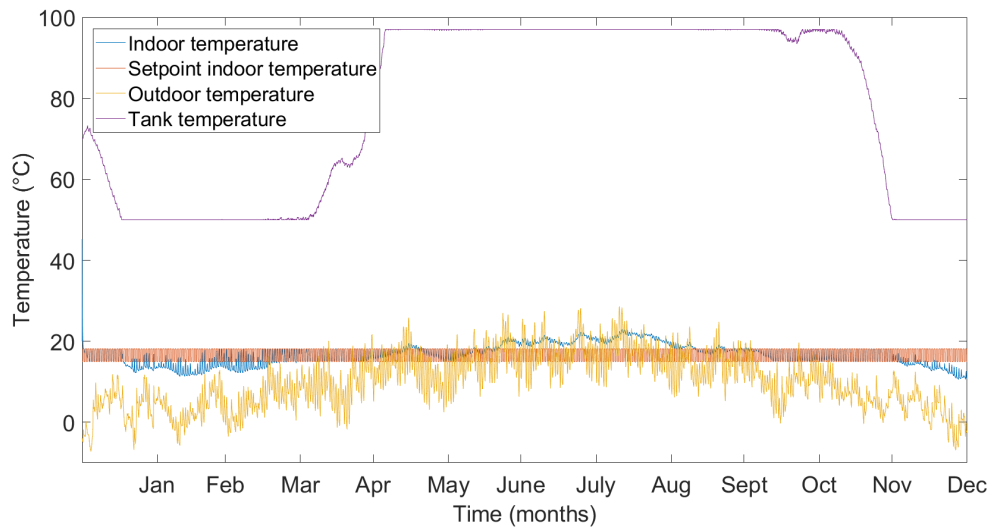


Figure C.11: The yearly temperature variation for 2 PVT panels and 2 m³ TESS capacity.

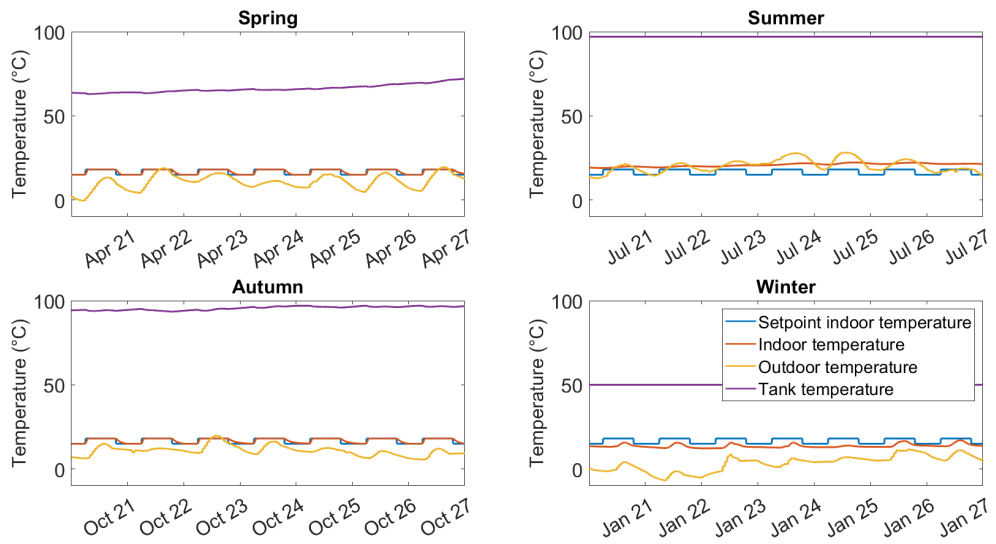


Figure C.12: The seasonal temperature variation for 2 PVT panels and 2 m³ TESS capacity.

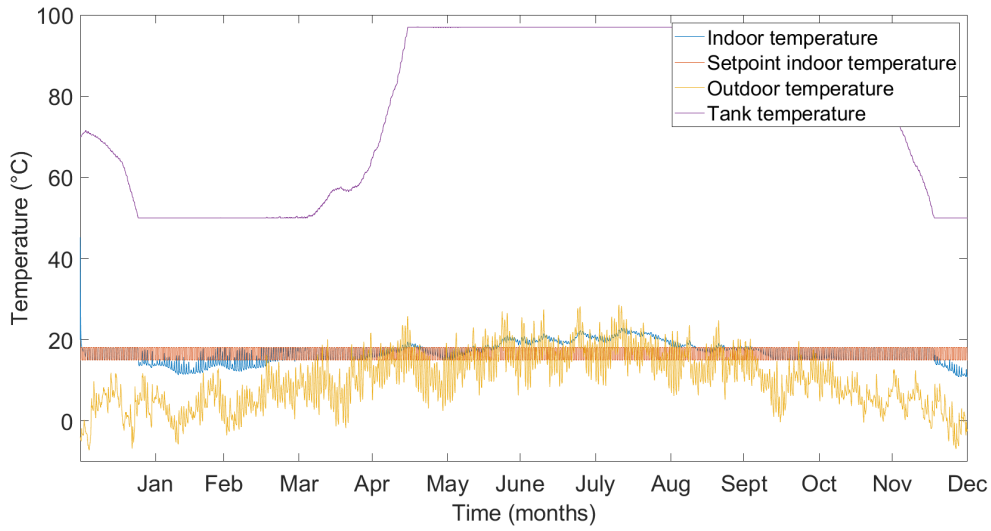


Figure C.13: The yearly temperature variation for 2 PVT panels and 4 m³ TESS capacity.

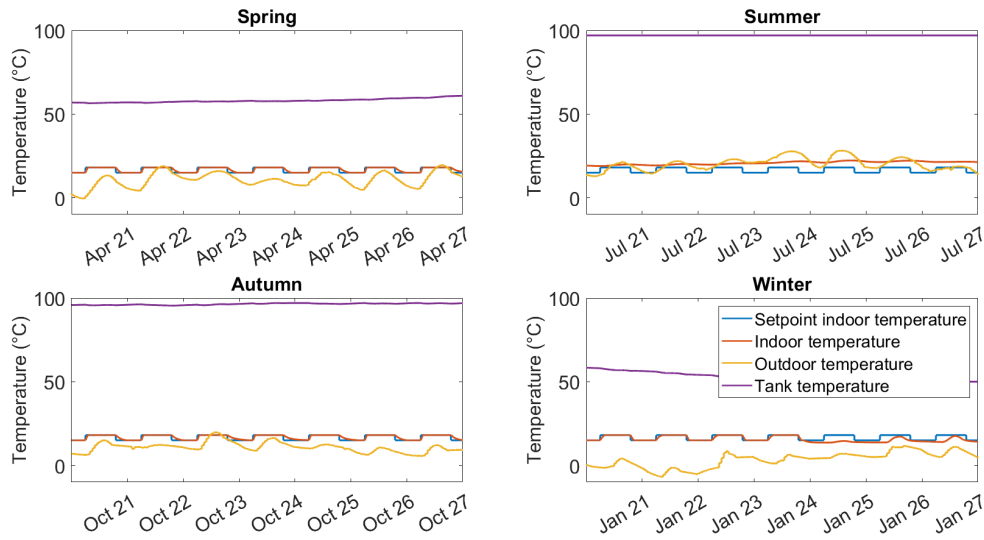


Figure C.14: The seasonal temperature variation for 2 PVT panels and 4 m³ TESS capacity.

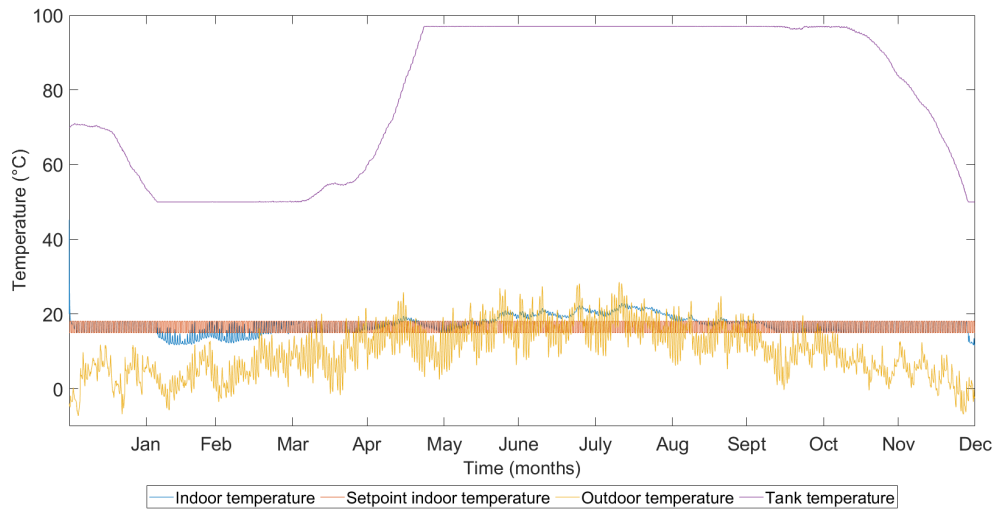


Figure C.15: The yearly temperature variation for 2 PVT panels and 6 m³ TESS capacity.

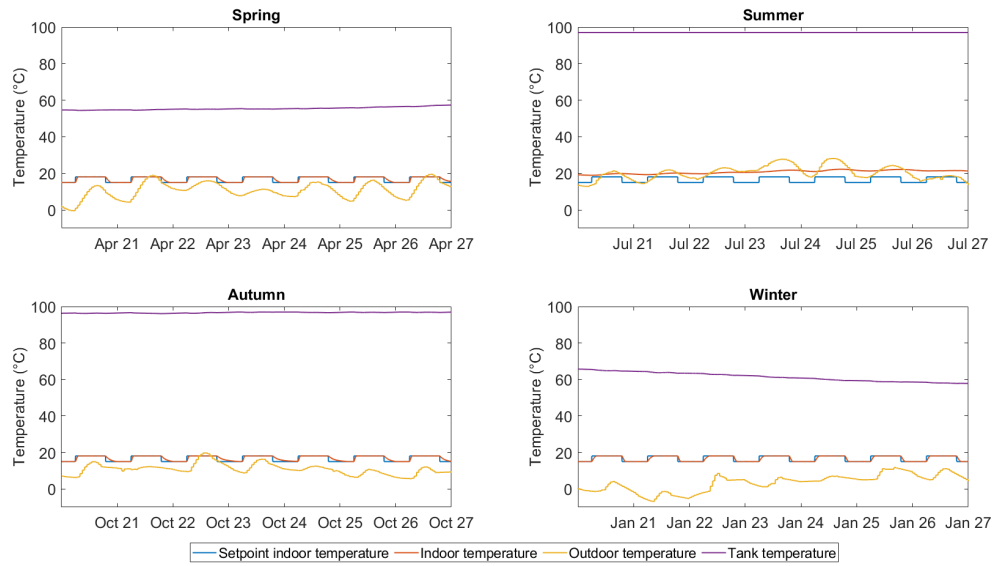


Figure C.16: The seasonal temperature variation for 2 PVT panels and 6 m³ TESS capacity.

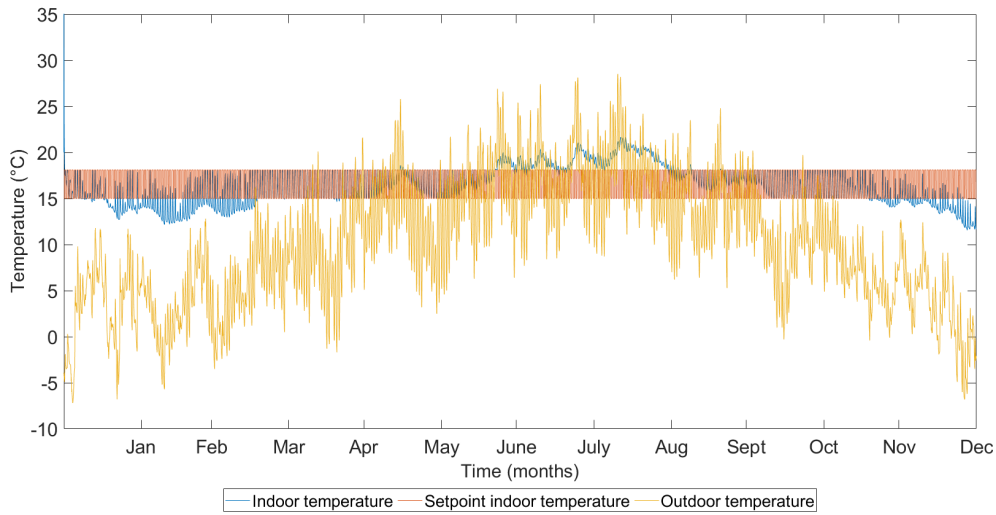


Figure C.17: The yearly temperature variation for 3 PVT panels and 0 m³ TESS capacity.

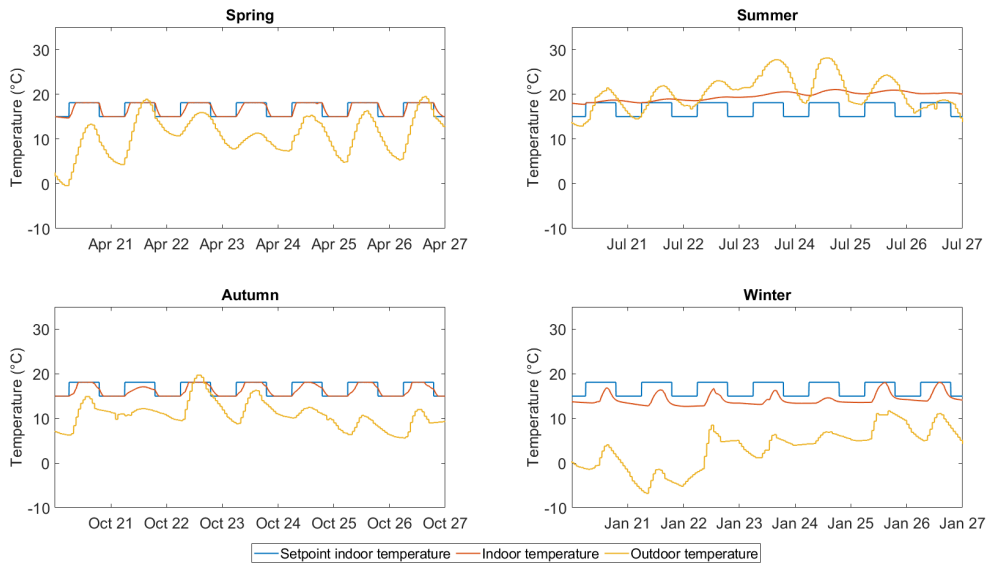


Figure C.18: The seasonal temperature variation for 3 PVT panels and 0 m³ TESS capacity.

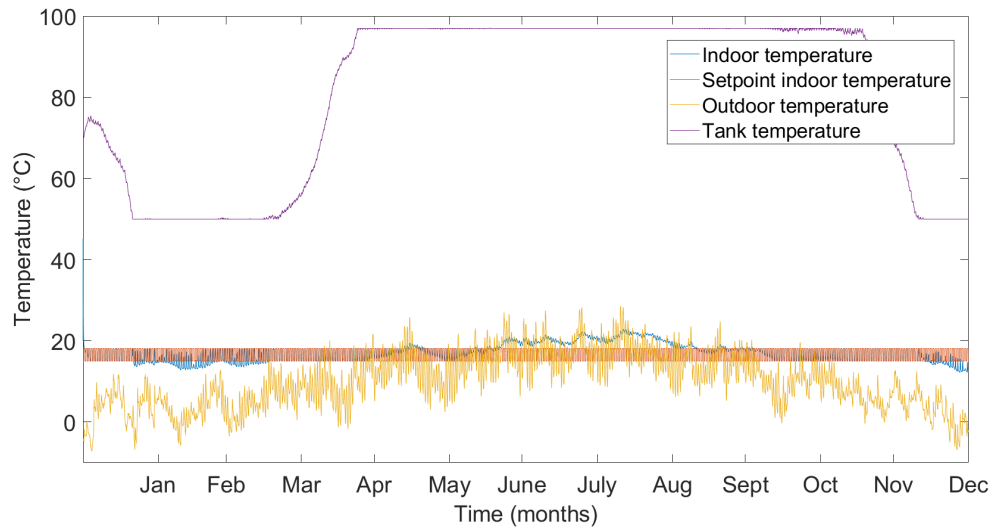


Figure C.19: The yearly temperature variation for 3 PVT panels and 2 m³ TESS capacity.

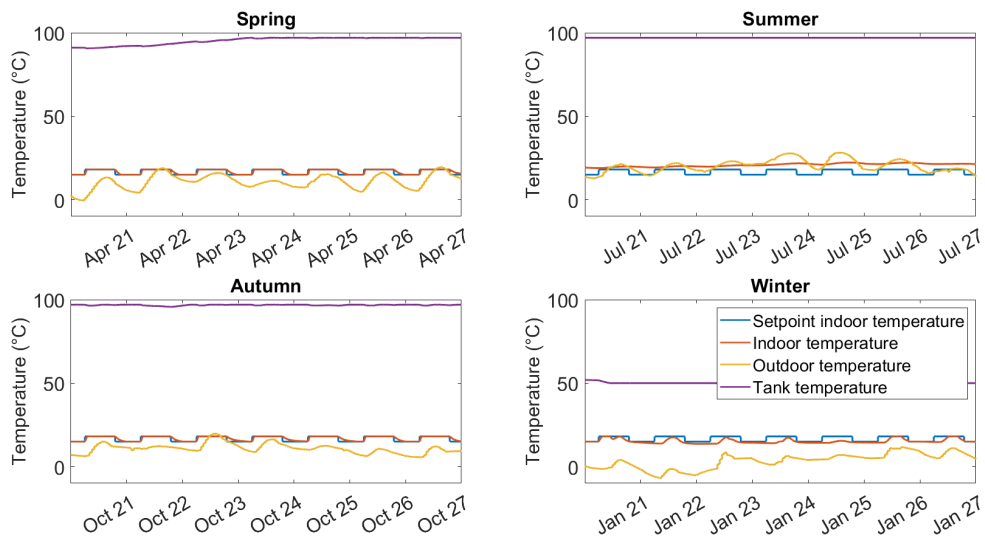


Figure C.20: The seasonal temperature variation for 3 PVT panels and 2 m³ TESS capacity.

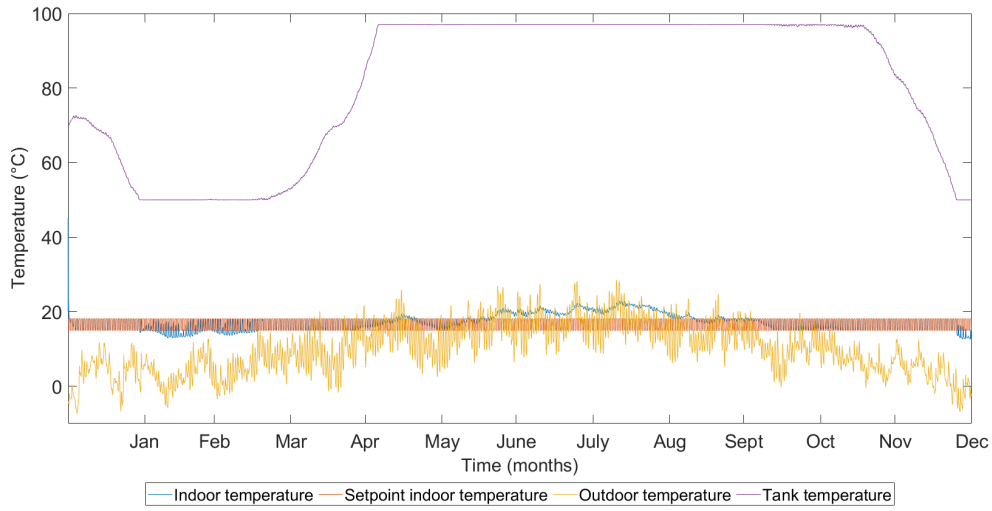


Figure C.21: The yearly temperature variation for 3 PVT panels and 4 m³ TESS capacity.

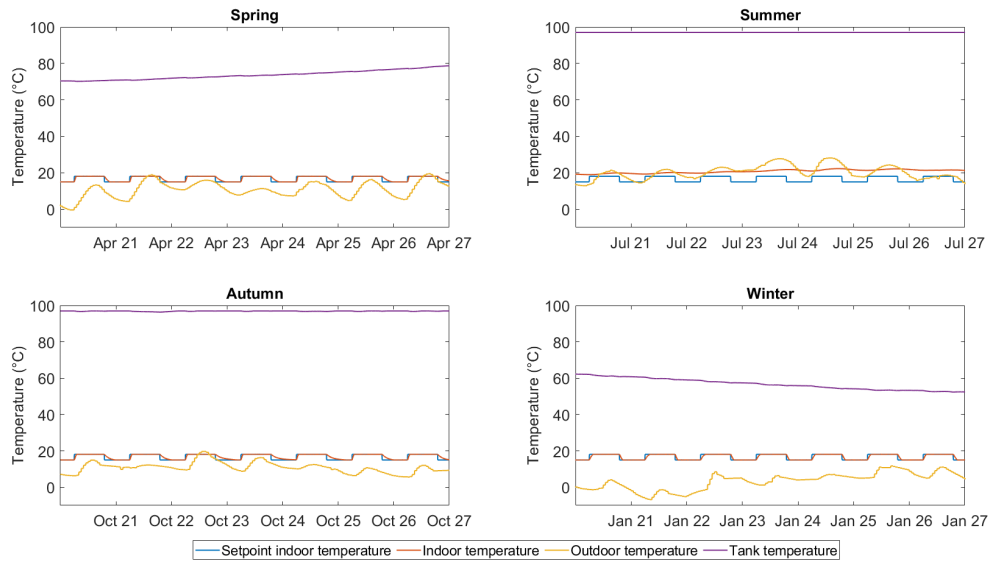


Figure C.22: The seasonal temperature variation for 3 PVT panels and 4 m³ TESS capacity.

D | ADDITIONAL RESULTS SCENARIO III

This appendix contains additional results of scenario III. In this scenario, the house is heated by a heat pump, a thermal energy buffer, and a PVT module.

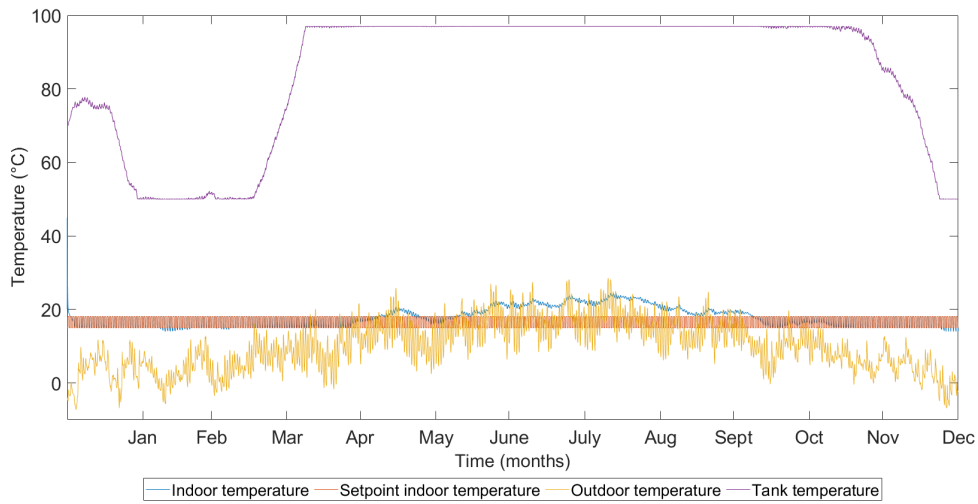


Figure D.1: The yearly temperature variation for 3 PVT panels, 2 m³ TESS capacity and a heat pump.

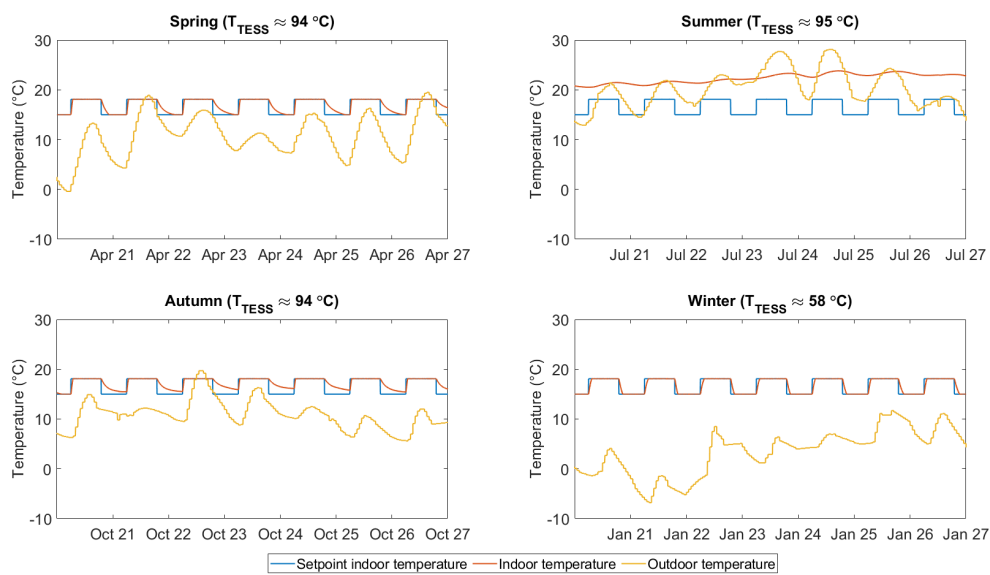


Figure D.2: The seasonal temperature variation for 3 PVT panels, 2 m³ TESS capacity and a heat pump.

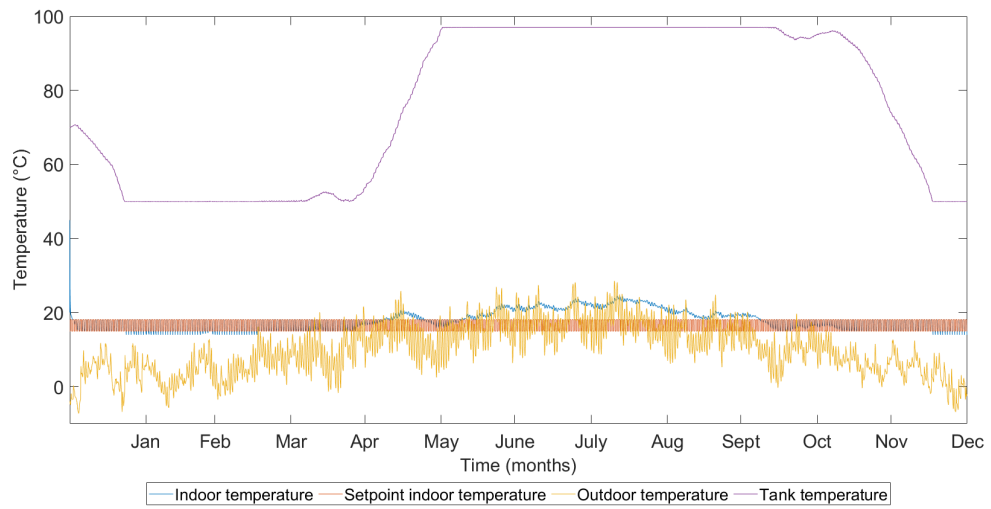


Figure D.3: The yearly temperature variation for 1 PVT panel, 4 m³ TESS capacity and a heat pump.

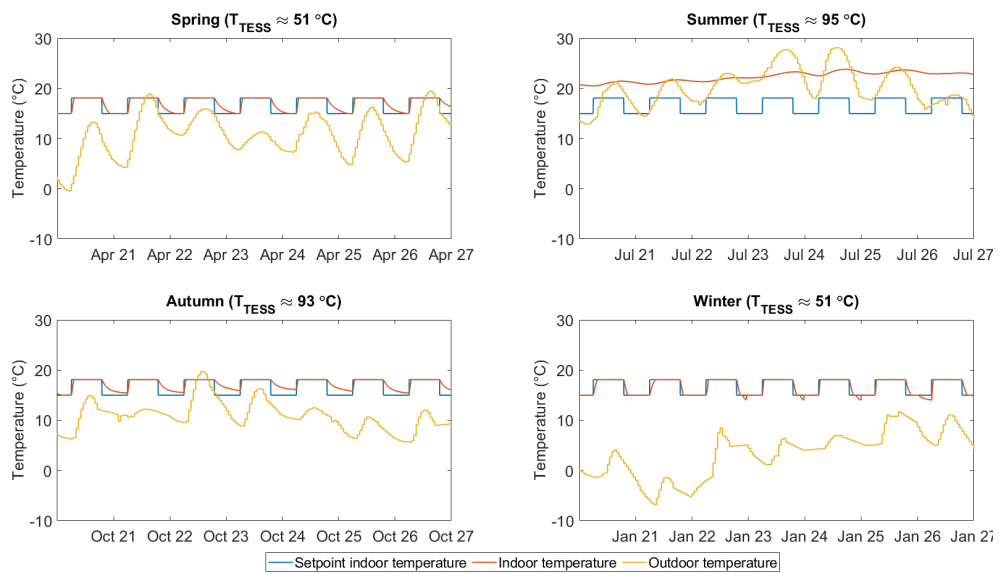


Figure D.4: The seasonal temperature variation for 1 PVT panel, 4 m³ TESS capacity and a heat pump.

E | PVT MODULE PARAMETERS

This appendix contains all defined parameters, such as the dimensions and material properties of the PVT module that was used in the simulations for this project. These parameters can be seen in Table E.1.

Table E.1: PVT module parameters

PVT module property	Value	Unit
Initial temperatures		
Glass cover	295	K
PV cells	295	K
Heat exchanger	295	K
Water in the tank	295	K
Back cover	295	K
Geometry		
Area of a cell	0.0225	m ²
Number of cells	72	-
Optical properties		
Refractive index ratio glass/air	1.52	-
Absorption coefficient of glass per unit length	0.2	1/m
Thickness of glass cover	0.01	m
Reflection factor of PV cell	0.15	-
Heat transfer properties		
Temperature of ambient air	295	K
Temperature of sky (for radiative heat transfer)	290	K
Mass of glass cover	4	kg
Mass of one PV cell	0.2	kg
Mass of heat exchanger	15	kg
Mass of back cover	5	kg
Specific heat of glass	800	J/kgK
Specific heat of PV cell	200	J/kgK
Specific heat of heat exchanger	460	J/kgK
Specific heat of back cover	400	J/kgK
Emissivity of glass	0.75	-
Emissivity of PV cell	0.7	-
Free convection coefficient between glass and ambient air	10	W/m ² K
Free convection coefficient between PV cells and glass	20	W/m ² K
Free convection coefficient between back cover and ambient air	10	W/m ² K
Thermal conductivity of heat exchanger	130	W/mK
Thickness of heat exchanger	0.04	m
Thermal conductivity of insulation layer	0.1	W/mK
Thickness of insulation layer	0.03	m
PV cell electrical properties		
Short-circuit current, I_{sc}	8.88	A
Open-circuit voltage, V_{oc}	0.62	V

Diode saturation current, Is	1.00e-06	A
Diode saturation current, Is2	0	A
Solar-generated current for measurements, Ipho	8.88	A
Irradiance used for measurements, Iro	1000	W/m ²
Quality factor, N	1.5	-
Quality factor, N2	2	-
Series resistance, Rs	0	Ω
Parallel resistance, Rp	∞	Ω
First order temperature coefficient for Iph, TIPH1	0	1/K
Energy gap, EG	1.11	eV
Temperature exponent for Is, TXIS1	3	-
Temperature exponent for Is2, TXIS2	3	-
Temperature exponent for Rs, TRS1	0	-
Temperature exponent for Rp, TRP1	0	-
Measurement temperature	25	°C
